BULLETIN OF THE EARTHQUAKE
RESEARCH INSTITUTE
Vol. 48 (1970), pp. 533-579

30. *Theoretical Seismograms and Earthquake Mechanism. Part I. Basic Principles. Part II. Effect of Time Function on Surface Waves.*

By Tatsuo USAMI,
Earthquake Research Institute,

Toshikazu ODAKA,
Geophysical Institute, the University of Tokyo,

and

Yasuo SATÔ,
Earthquake Research Institute.

(Read March 24, 1970.—Received May 31, 1970.)

Contents

Introduction

Since a theoretical seismogram was first calculated for the torsional disturbances on the surface of a homogeneous elastic sphere [Satô et al. (1962)], it has become one of the powerful tools of studying focal mechanisms and of interpreting various phases recorded on actual seismograms. Works by Kanamori (1970a, 1970b) and Chander et al. (1968) are the most recent ones along this line. In these studies, however, disturbances with a limited period range are synthesized assuming source mechanisms appropriate for their own purposes. On the other hand, theoretical seismograms calculated by the present authors cover a wide range of period from that of the gravest mode to about 10 seconds, and a stress was assumed on the free surface or on a surface within the earth [Satô et al. (1968, 1970), Usami et al. (1970)]. These situations inevitably lead the authors to the study of the effect of source mechanism to body and surface waves found in theoretical seismograms.

The theoretical aspects of the calculation of disturbances due to various kinds of force systems at the source region have been given by Saito (1967), Singh and Ben-Menahem (1969a, 1969b) and R. Sato (1969) in elegant forms. In the present paper, a similar problem was pursued using somewhat different methods with special attention to the contribution of P, $S1$ and $S2$ waves to the resulting disturbances. Convenient expressions for computing theoretical seismograms are also given for typical kinds of force systems. This series of papers, the present one being the first, intends to prepare seismograms expected on the surface of the earth for various kinds of focal mechanism. It is also intended to furnish the first approximation of the mechanism of earthquake by the comparison of the actual seismograms with the theoretical ones.

Part I. Basic Principles

A. Expression of Source Function

§ 1.1 Expression of Displacement due to Body Force

Expression of displacement in a homogeneous elastic medium due to

a body force applied within the medium is given in the famous book by A. E. H. Love (1934). Body force per unit mass K and displacement U are expressed as

$$\left.\begin{aligned} K&=\mathrm{grad}\,\phi+\mathrm{rot}\cdot\mathrm{rot}\,\boldsymbol{\psi}\\ U&=\mathrm{grad}\,\Phi+\mathrm{rot}\cdot\mathrm{rot}\,\boldsymbol{\Psi}\end{aligned}\right\} \qquad (1\cdot1\cdot1)$$

and they are related to each other through the equation of motion, namely,

$$(\lambda+2\mu)\,\mathrm{grad}\cdot\mathrm{div}\,U-\mu\,\mathrm{rot}\cdot\mathrm{rot}\,U+\rho K=\rho\frac{\partial^2}{\partial t^2}U \qquad (1\cdot1\cdot2)$$

Displacement U is derived from the solutions of the equations

$$\left.\begin{aligned} &(\lambda+2\mu)\nabla^2\Phi+\rho\phi=\rho\frac{\partial^2}{\partial t^2}\Phi\\ &-\mu\,\mathrm{rot}\cdot\mathrm{rot}\,\boldsymbol{B}+\rho\boldsymbol{A}=\rho\frac{\partial^2}{\partial t^2}\boldsymbol{B}\end{aligned}\right\} \qquad (1\cdot1\cdot3)$$

where

$$\boldsymbol{A}=\mathrm{rot}\,\boldsymbol{\psi}\,,\qquad \boldsymbol{B}=\mathrm{rot}\,\boldsymbol{\Psi}\,. \qquad (1\cdot1\cdot4)$$

The solutions of the equations (1·1·3) are

$$\left.\begin{aligned} \Phi&=\frac{1}{4\pi V_P{}^2}\iiint_v\frac{1}{r}\phi(t-r/V_P)\,dv\\ \boldsymbol{B}&=\frac{1}{4\pi V_S{}^2}\iiint_v\frac{1}{r}\boldsymbol{A}(t-r/V_S)\,dv\end{aligned}\right\} \qquad (1\cdot1\cdot5)$$

V_P and V_S are the velocities of P and S waves and the integral covers all space v. r is the distance to a point in v.

It is well known that scalar ϕ and vector $\boldsymbol{A}$ are expressed as

$$\left.\begin{aligned} \phi&=-\frac{1}{4\pi}\iiint\frac{1}{R}\cdot(\mathrm{div}'K)\,dv'=\frac{1}{4\pi}\iiint\left[\mathrm{grad}'\left(\frac{1}{R}\right)\cdot K\right]dv'\\ \boldsymbol{A}&=\frac{1}{4\pi}\iiint\frac{1}{R}(\mathrm{rot}'K)\,dv'=-\frac{1}{4\pi}\iiint\left[\mathrm{grad}'\left(\frac{1}{R}\right)\times K\right]dv'\end{aligned}\right\} \qquad (1\cdot1\cdot6)$$

Notation $(')$ on the upper right of differential operators means the differentiation with respect to a point (x', y', z') in the volume v'. All the forces applied are included in the volume v'.

Employing a function $\mathrm{F}(t)$ introduced by Keilis-Borok (1950)

$$\mathbf{F}(t)=\int^{t}dt''\int^{t''}\boldsymbol{K}(t')dt', \tag{1·1·7}$$

the function $\boldsymbol{I}(t)$ which will appear in the integral expression of Φ and $\boldsymbol{B}$ is

$$\begin{aligned}\boldsymbol{I}(t,V_P)&=\int_0^{r/V_P}t'\boldsymbol{K}(t-t')dt'=\int_0^{r/V_P}\boldsymbol{K}(t-t')dt'\int_0^{t'}ds\\&=-\mathbf{F}(t-r/V_P)+\mathbf{F}(t)-\frac{r}{V_P}\mathbf{F}'(t-r/V_P)\end{aligned} \tag{1·1·8}$$

Putting the relation (1.1.6) into (1.1.4), the scalar and vector potentials expressing the displacement due to a body force $\boldsymbol{K}$ distributed in the volume v' are obtained as

$$\left.\begin{aligned}\Phi&=\frac{1}{4\pi}\iiint\left[\operatorname{div}\left(\frac{1}{r_0}\cdot\mathbf{F}(t-r_0/V_P)\right)-\operatorname{grad}\left(\frac{1}{r_0}\right)\cdot\mathbf{F}(t)\right]dv'\\\boldsymbol{B}&=-\frac{1}{4\pi}\iiint\left[\operatorname{rot}\left(\frac{1}{r_0}\cdot\mathbf{F}(t-r_0/V_S)\right)-\operatorname{grad}\left(\frac{1}{r_0}\right)\times\mathbf{F}(t)\right]dv'\end{aligned}\right\} \tag{1·1·9}$$

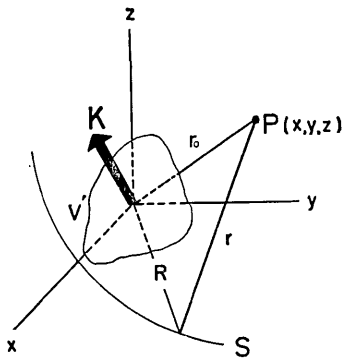

Fig. 1.

In deriving this formula, the relation (1.1.8) and the following integral were used

$$\iint_S\operatorname{grad}'\left(\frac{1}{R}\right)dS=\begin{cases}0 & r_0<r\\-4\pi r^2\operatorname{grad}\left(\dfrac{1}{r_0}\right) & r_0>r\end{cases} \tag{1·1·10}$$

The notations r_0, R and r are seen in Figure 1 and S is the spherical surface of radius r from the observation point $P(x, y, z)$.

When the external force is concentrated at the origin, $\boldsymbol{K}_0$ is defined by

$$\boldsymbol{K}_0=\rho\iiint_{v'}\boldsymbol{K}dv' \tag{1·1·11}$$

and the formula (1.1.9) is reduced to

$$\left.\begin{aligned}\Phi&=\frac{1}{4\pi\rho}\left[\operatorname{div}\left(\frac{1}{r_0}\cdot\mathbf{F}_0(t-r_0/V_P)\right)-\operatorname{grad}\left(\frac{1}{r_0}\right)\cdot\mathbf{F}_0(t)\right]\\\boldsymbol{B}&=-\frac{1}{4\pi\rho}\left[\operatorname{rot}\left(\frac{1}{r_0}\cdot\mathbf{F}_0(t-r_0/V_S)\right)-\operatorname{grad}\left(\frac{1}{r_0}\right)\times\mathbf{F}_0(t)\right]\end{aligned}\right\} \tag{1·1·12}$$

where

$$F_0(t)=\int^{t} dt''\int^{t''} K_0(t')dt' \qquad (1\cdot1\cdot13)$$

§ 1.2 Force System and Expression of Potentials

General solutions of vector and scalar displacement potentials due to arbitrary force systems were obtained in the previous section and they will be applied to the force systems of special interest. In this section, a point source is assumed at the origin and the formula (1.1.12) is employed. Solutions for a force system distributed within a volume v' will be obtained by integrating the solutions for a concentrated force over this region.

The displacement is given by

$$\boldsymbol{U}=\mathrm{grad}\,\Phi+\mathrm{rot}\,\boldsymbol{B} \qquad (1\cdot2\cdot1)$$

Since $F_0(t)$ is a function of coordinate (x', y', z') and not of (x, y, z), the rotation and divergence of $F_0(t)$ with respect to the latter coordinate system vanish. Therefore, the contributions of the scalar and vector potentials to displacement from the second terms of the right-hand side of the equations (1·1·12) cancel each other. Thus, these terms will be disregarded in this study.

a) Single Force. We assume that

$$F_0(t)=\boldsymbol{1}_0\cdot F_A\cdot F(t) \qquad (1\cdot2\cdot2)$$

where $\boldsymbol{1}_0$ is the unit vector in the direction of applied force, and F_A the magnitude of applied force. A polar coordinate referred to the Cartesian coordinate (x, y, z) is introduced. The direction of a unit vector $\boldsymbol{1}_0$ is expressed by (θ_0', φ_0') and the position of observation point by $(r_0, \theta_0, \varphi_0)$.

Then we have

$$\Phi=\frac{F_A}{4\pi\rho}[\cos\theta_0\cdot\cos\theta_0'+\sin\theta_0\cdot\sin\theta_0'\cdot\cos(\varphi_0-\varphi_0')]\cdot\frac{d}{dr_0}G(V_P) \qquad (1\cdot2\cdot3)$$

where $G(V_P)$ stands for $(1/r_0)\cdot F(t-r_0/V_P)$. The vector potential $\boldsymbol{B}$ is expressed by

$$\boldsymbol{B}=-\frac{F_A}{4\pi\rho}\,\mathrm{rot}\left\{H,\ \frac{\partial H}{\partial\theta_0},\ \frac{1}{\sin\theta}\frac{\partial H}{\partial\varphi_0}\right\}_{r_0}\cdot G(V_S)$$
$$H=\sin\theta_0\cdot\sin\theta_0'\cdot\cos(\varphi_0-\varphi_0') \qquad (1\cdot2\cdot4)$$

Suffix r_0 represents the polar coordinate $(r_0, \theta_0, \varphi_0)$ and the notation

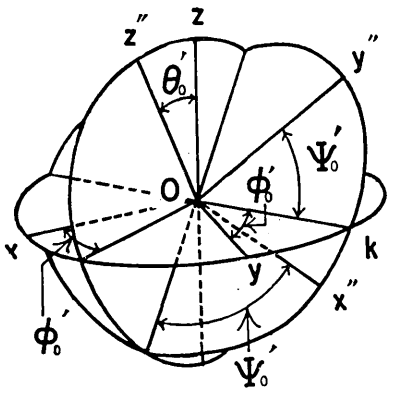

Fig. 2. Relation between coordinate systems (x, y, z) and (x'', y'', z''). The former is nothing but the (x, y, z) system in Figure 1 referred to the source point, the latter being introduced to give simpler expressions to force system.

$\{\ \}_{r_0}$ means that the expressions inside are the components of a vector referred to this coordinate system.

b) Single Couple. A rectangular coordinate (x'', y'', z'') is introduced as shown in Figure 2. This system is related to the original one (x, y, z) through Eulerian angles φ_0', θ_0', ϕ_0'. The former is obtained by rotating the latter around z axis by φ_0', around Ok by θ_0' and around z'' axis by ϕ_0'. The direction cosines between the axes of two systems are

	x	y	z
x''	$\cos\varphi_0'\cdot\cos\theta_0'\cdot\cos\phi_0'$ $-\sin\varphi_0'\cdot\sin\phi_0'$	$\sin\varphi_0'\cdot\cos\theta_0'\cdot\cos\phi_0'$ $+\cos\varphi_0'\cdot\sin\phi_0'$	$-\sin\theta_0'\cdot\cos\phi_0'$
y''	$-\cos\varphi_0'\cdot\cos\theta_0'\cdot\sin\phi_0'$ $-\sin\varphi_0'\cdot\cos\phi_0'$	$-\sin\varphi_0'\cdot\cos\theta_0'\cdot\sin\phi_0'$ $+\cos\varphi_0'\cdot\cos\phi_0'$	$\sin\theta_0'\cdot\sin\phi_0'$
z''	$\sin\theta_0'\cdot\cos\varphi_0'$	$\sin\theta_0'\cdot\sin\varphi_0'$	$\cos\theta_0'$

(1·2·5)

Assuming a single couple force in the $x''-y''$ plane as in Figure 3, the function corresponding to $\frac{1}{r_0}F_0\left(t-\frac{r_0}{V_P}\right)$ in the expressions (1·1·12) becomes

$$-\frac{\partial}{\partial y''}\left\{\frac{1}{r_0}F_0\left(t-\frac{r_0}{V_P}\right)\right\}\cdot\delta y''=-\frac{\partial}{\partial y''}\left\{\frac{1}{r_0}1_0\cdot M_0\cdot F\left(t-\frac{r_0}{V_P}\right)\right\} \qquad (1\cdot2\cdot6)$$

where M_0 is the moment of a single couple, namely,

$$M_0 = F_A \cdot \delta y''$$

Equation (1·2·6) is reduced to

$$= -\mathbf{1}_0 \cdot \frac{\partial}{\partial y''} \{G(V_P)\} \cdot M_0 \qquad (1\cdot2\cdot7)$$

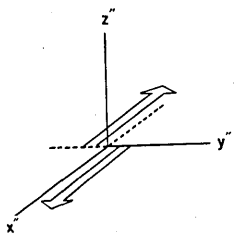

Fig. 3. Single couple force system in the $x''-y''$ plane.

Since $G(V_P)$ is a function of r_0 only, this can be written as

$$= -M_0 \cdot \mathbf{1}_0 \cdot \Omega \cdot \frac{d}{dr_0} G(V_P)$$

$$\Omega = \sin\theta_0 \cdot \cos\psi_0' \cdot \sin(\varphi_0 - \varphi_0') + \sin\psi_0' (\cos\theta_0 \cdot \sin\theta_0' - \sin\theta_0 \cdot \cos\theta_0' \cdot \cos(\varphi_0 - \varphi_0')) \qquad (1\cdot2\cdot8)$$

Therefore, the scalar and vector potentials for a single couple are readily obtained by putting (1·2·8) into (1·1·12).

$$\left.\begin{aligned} \Phi &= -\frac{M_0}{4\pi\rho} \cdot \Omega \cdot R_1 \cdot \left\{ \frac{d^2}{dr_0^2} G(V_P) - \frac{1}{r_0} \frac{d}{dr_0} G(V_P) \right\} \\ \boldsymbol{B} &= \frac{M_0}{4\pi\rho} \cdot \mathrm{rot} \left\{ R_1 \Omega,\ \frac{\partial R_1}{\partial \theta_0} \Omega,\ \frac{1}{\sin\theta_0} \frac{\partial R_1}{\partial \varphi_0} \Omega \right\}_{r_0} \cdot \frac{d}{dr_0} G(V_S) \end{aligned}\right\} \qquad (1\cdot2\cdot9)$$

$$\begin{aligned} R_1 = {} & \sin\theta_0 \cdot \cos\theta_0' \cdot \cos\psi_0' \cdot \cos(\varphi_0 - \varphi_0') \\ & - \cos\theta_0 \cdot \sin\theta_0' \cdot \cos\psi_0' \\ & + \sin\theta_0 \cdot \sin\psi_0' \cdot \sin(\varphi_0 - \varphi_0') \end{aligned} \qquad (1\cdot2\cdot10)$$

c) Dip Slip. First, two coordinate systems (x_1, x_2, x_3) and $(\bar{x}, \bar{y}, \bar{z})$ as shown in Figure 4 are introduced. The direction of strike of a fault plane is given by the angle γ measured from the x-axis and the dip angle δ is defined as in the Figure 4. x_1-axis is taken as the direction of the strike, x_2-axis perpendicular to x_1-axis lying in the fault plane and x_3-axis is perpendicular to the fault plane. In the coordinate system (x_1, x_2, x_3),

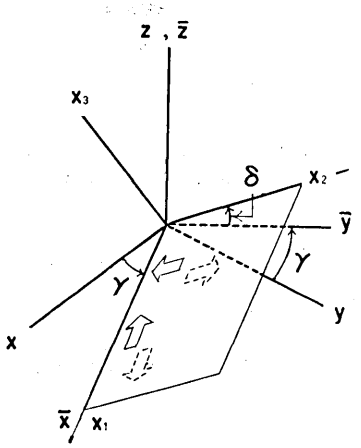

Fig. 4. Double couple force system associated with dip and strike slip faults. γ is the direction of the strike and δ the dip angle. The coordinate system (x_1, x_2, x_3) is referred to the fault, the x_1-x_2 plane meaning the fault plane. Arrows show the force system associated with the dip and strike slip faults.

two single couple forces are assumed as shown in Figure 5, making a double couple associated with dip slip fault of strike direction γ and dip angle δ. Referring to the former paragraph, single couple force specified by notation (I) in Figure 5, is expressed by

$$\varphi_0'=\gamma, \qquad \theta_0'=-\pi/2, \qquad \psi_0'=-\pi/2-\delta \tag{1·2·11}$$

and for the one with notation (II), the Eulerian angles are

$$\varphi_0'=\gamma-\pi, \qquad \theta_0'=-\pi/2, \qquad \psi_0'=\delta \tag{1·2·12}$$

The combined effect of the two single couples gives

$$\left.\begin{aligned} \Phi&=-\frac{M_0}{4\pi\rho}\cdot R_d\cdot\left\{\frac{d^2}{dr_0^2}G(V_P)-\frac{1}{r_0}\frac{d}{dr_0}G(V_P)\right\} \\ \boldsymbol{B}&=\frac{M_0}{4\pi\rho}\cdot\mathrm{rot}\left\{R_d,\ \frac{1}{2}\frac{\partial R_d}{\partial\theta_0},\ \frac{1}{2\sin\theta_0}\frac{\partial}{\partial\varphi_0}R_d\right\}_{r_0}\cdot\frac{d}{dr_0}G(V_S) \end{aligned}\right\} \tag{1·2·13}$$

$$R_d=-\cos 2\delta\cdot\sin 2\theta_0\cdot\sin(\varphi_0-\gamma)-\sin 2\delta\cdot(\cos^2\theta_0-\sin^2\theta_0\cdot\sin^2(\varphi_0-\gamma)) \tag{1·2·14}$$

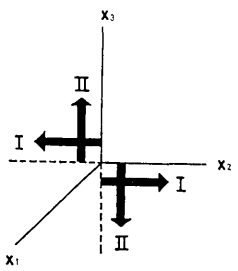

Fig. 5. Force system associated with dip slip fault. x_1-x_2 plane is the fault plane.

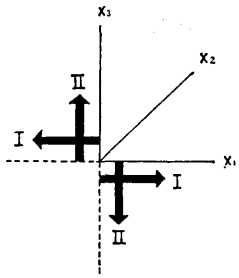

Fig. 6. Force system associated with strike slip fault. x_1-x_2 plane means the fault plane.

d) Strike Slip. The directions of strike and dip angle are defined in the same way as the case of dip slip. Two single couples referred to (x_1, x_2, x_3) are assumed as in Figure 6. In this case, the single couple forces (I) and (II) are specified by Eulerian angles

$$\left.\begin{aligned} &\text{(I)} \quad \varphi_0'=\gamma-\pi/2, \quad \theta_0'=-\pi/2+\delta, \quad \psi_0'=-\pi/2 \\ &\text{(II)} \quad \varphi_0'=\gamma+\pi/2, \quad \theta_0'=-\pi/2-\delta, \quad \psi_0'=0 \end{aligned}\right\} \tag{1·2·15}$$

The vector and scalar potentials have the expressions

$$\left.\Phi=-\frac{M_0}{4\pi\rho}\cdot R_s\cdot\left\{\frac{d^2}{dr_0^2}G(V_P)-\frac{1}{r_0}\frac{d}{dr_0}G(V_P)\right\}\right. \tag{1·2·16}$$

$$\left.\begin{aligned} \boldsymbol{B}&=\frac{M_0}{4\pi\rho}\cdot\mathrm{rot}\left\{R_s,\ \frac{1}{2}\frac{\partial}{\partial\theta_0}R_s,\ \frac{1}{2\sin\theta_0}\frac{\partial}{\partial\varphi_0}R_s\right\}_{r_0}\cdot\frac{d}{dr_0}G(V_S)\\ R_s&=-\cos\delta\cdot\sin 2\theta_0\cdot\cos(\varphi_0-\gamma)+\sin\delta\cdot\sin^2\theta_0\cdot\sin 2(\varphi_0-\gamma)\end{aligned}\right\}\quad(1\cdot2\cdot17)$$

§ 1.3 Further Reduction for Harmonic Source

(a) When the applied force $K(t)$ is proportional to $\exp(jpt)$ we have from the relations (1.1.13) and (1.2.2)

$$F(t)=-\exp(jpt)/p^2$$

where j is the unit of imaginary number. Function G and its derivatives can be calculated as follows

$$\left.\begin{aligned} G(V_P)&=\frac{1}{r_0}F(t-r_0/V_P)=\frac{j}{pV_P}h_0^{(2)}(pr_0/V_P)\cdot\exp(jpt)\\ \frac{d}{dr_0}G(V_P)&=-\frac{j}{V_P^2}h_1^{(2)}(pr_0/V_P)\cdot\exp(jpt)\\ \frac{d^2}{dr_0^2}G(V_P)-\frac{1}{r_0}\frac{d}{dr_0}G(V_P)&=\frac{jp}{V_P^3}h_2^{(2)}(pr_0/V_P)\cdot\exp(jpt)\end{aligned}\right\}\quad(1\cdot3\cdot2)$$

Corresponding functions for $G(V_S)$ have similar expressions.

(b) For a polar coordinate system (r, θ, φ), the following relation is well-known.

$$\left.\begin{aligned} &\mathrm{rot}\left\{Q,\ \frac{1}{N}\frac{\partial Q}{\partial\theta},\ \frac{1}{N\sin\theta}\frac{\partial Q}{\partial\varphi}\right\}_r\\ &=\left\{0,\ \frac{1}{r\sin\theta}\frac{\partial}{\partial\varphi}\left(Q-\frac{1}{N}\frac{\partial}{\partial r}(rQ)\right),\ -\frac{1}{r}\frac{\partial}{\partial\theta}\left(Q-\frac{1}{N}\frac{\partial}{\partial r}(rQ)\right)\right\}_r\\ &=\mathrm{rot}\left\{Q-\frac{1}{N}\frac{\partial}{\partial r}(rQ),\ 0,\ 0\right\}_r\end{aligned}\right\}\quad(1\cdot3\cdot3)$$

where N is a constant.

(c) Using the formulas (1·3·2) and (1·3·3), the scalar and vector potentials for various kinds of force systems treated in the former sections can be reduced to simpler forms.

They are:

Single force

$$\left.\begin{aligned} \Phi&=\frac{-jF_A\cdot e^{jpt}}{4\pi\rho V_P^2}\cdot\Lambda\cdot h_1^{(2)}(pr_0/V_P),\\ \boldsymbol{B}&=\frac{-jF_A\cdot e^{jpt}}{4\pi\rho V_S^2}\cdot\mathrm{rot}\{r_0\Lambda\cdot h_1^{(2)}(pr_0/V_S),\ 0,\ 0\}_{r_0}\\ \Lambda&=\cos\theta_0'\cdot P_1(\cos\theta_0)+\sin\theta_0'\cdot P_1^1(\cos\theta)\cdot\cos(\varphi_0-\gamma)\end{aligned}\right\}\quad(1\cdot3\cdot4)$$

Single couple

$$\left.\begin{aligned}\Phi&=\frac{-jpM_0e^{jpt}}{4\pi\rho V_P^{\,3}}\Lambda\cdot h_2^{(2)}(pr_0/V_P)\\ \boldsymbol{B}&=\frac{-jpM_0e^{jpt}}{8\pi\rho V_S^{\,3}}\cdot\mathrm{rot}\{r_0\Lambda\cdot h_2^{(2)}(pr_0/V_S),\,0,\,0\}_{r_0}\\ &\quad+\frac{jM_0e^{jpt}}{8\pi\rho V_S^{\,2}}\mathrm{rot}\cdot\mathrm{rot}\{r_0\bar{\Lambda}\cdot h_1^{(2)}(pr_0/V_S),\,0,\,0\}_{r_0}\end{aligned}\right\}\qquad(1\cdot3\cdot5)$$

$$\left.\begin{aligned}\Lambda&=\cos 2\phi_0'\cdot\left\{\frac{1}{6}P_2^2(\cos\theta_0)\cdot\cos\theta_0'\cdot\sin 2(\varphi_0-\gamma)\right.\\ &\quad\left.-\frac{1}{3}P_2^1(\cos\theta)\cdot\sin\theta_0'\cdot\sin(\varphi_0-\gamma)\right\}\\ &\quad+\sin 2\phi_0'\cdot\left\{-\frac{1}{12}P_2^2(\cos\theta_0)\cdot(1+\cos^2\theta_0')\cdot\cos 2(\varphi_0-\gamma)\right.\\ &\quad\left.+\frac{1}{6}P_2^1(\cos\theta_0)\cdot\sin 2\theta_0'\cdot\cos(\varphi_0-\gamma)-\frac{1}{2}P_2(\cos\theta_0)\cdot\sin^2\theta_0'\right\}\\ \bar{\Lambda}&=P_1(\cos\theta_0)\cdot\cos\theta_0'+P_1^1(\cos\theta_0)\cdot\sin\theta_0'\cdot\cos(\varphi_0-\gamma)\end{aligned}\right\}\qquad(1\cdot3\cdot6)$$

Dip slip

$$\left.\begin{aligned}\Phi&=-\frac{jpM_0}{4\pi\rho V_P^{\,3}}e^{jpt}\Lambda\cdot h_2^{(2)}(pr_0/V_P)\\ \boldsymbol{B}&=-\frac{jpM_0}{8\pi\rho V_S^{\,3}}e^{jpt}\cdot\mathrm{rot}\{r_0\Lambda\cdot h_2^{(2)}(pr_0/V_S),\,0,\,0\}_{r_0}\end{aligned}\right\}\qquad(1\cdot3\cdot7)$$

$$\begin{aligned}\Lambda=R_d=&-\frac{2}{3}P_2^1(\cos\theta_0)\cdot\cos 2\delta\cdot\sin(\varphi_0-\gamma)\\ &-\sin 2\delta\cdot\left(P_2(\cos\theta_0)+\frac{1}{6}P_2^2(\cos\theta_0)\cdot\cos 2(\varphi_0-\gamma)\right)\end{aligned}\qquad(1\cdot3\cdot8)$$

Strike slip

The same as the case of dip slip with the exception of

$$\begin{aligned}\Lambda=R_s=&-\frac{2}{3}P_2^1(\cos\theta_0)\cdot\cos\delta\cdot\cos(\varphi_0-\gamma)\\ &+\frac{1}{3}P_2^2(\cos\theta_0)\cdot\sin\delta\cdot\sin 2(\varphi_0-\gamma)\end{aligned}\qquad(1\cdot3\cdot9)$$

B. Transformation of Coordinate Systems

§ 1.4 Coordinate Systems

Cartesian coordinate system $(\overline{X},\ \overline{Y},\ \overline{Z})$ fixed to the earth's center is

introduced as shown in Figure 7. $\bar{Z}$-axis is directed to the north and $\bar{X}$ and $\bar{Y}$ axes are on the equatorial plane and their longitudes are 0° and 90° respectively. The coordinate system (X, Y, Z) can be obtained by rotating the $(\bar{X}, \bar{Y}, \bar{Z})$ system as shown in the figure. An earthquake source is assumed to be on the Z axis. Another coordinate system (x, y, z) fixed to the focus is introduced in which x, y and z axes are parallel to X, Y and Z axes respectively. Thus it is seen that the x axis is directed southward, y eastward and z upward. This is nothing but the system used in the previous sections.

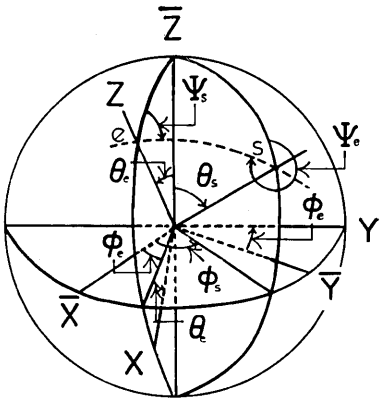

Fig. 7. Relation between coordinate systems. (X, Y, Z) system is fixed at the center of the earth and the Z axis is directed to the north. e is the focus and s the observation point. The system (X, Y, Z) is obtained by rotating the $(\bar{X}, \bar{Y}, \bar{Z})$ system around $\bar{Z}$ axis by φ_e and around Y axis by θ_e. Z axis directs to the focus.

Remembering that the suffixes e and s mean the quantities referred to the source and observation station respectively, the epicentral distance Δ is given by

$$\cos\Delta=\cos\theta_s\cdot\cos\theta_e+\sin\theta_s\cdot\sin\theta_e\cdot\cos(\varphi_e-\varphi_s) \qquad (1\cdot4\cdot1)$$

where φ is the longitude and $\pi/2-\theta$ the latitude. The azimuth of the source Ψ_e and station Ψ_s seen from the station and source respectively can be calculated from

$$-\frac{\sin\Psi_e}{\sin\theta_e}=\frac{\sin(\varphi_s-\varphi_e)}{\sin\Delta}=\frac{\sin\Psi_s}{\sin\theta_s} \qquad (1\cdot4\cdot2)$$

Position of station (Θ, Φ) expressed by a polar coordinate referred to the system (X, Y, Z) is given by

$$\Theta=\Delta, \qquad \Phi=\pi-\Psi_s \qquad (1\cdot4\cdot3)$$

Hereafter, all the discussions will be made referring to the coordinate (X, Y, Z).

§ 1.5 Transformation of Scalar and Vector Potentials from (x, y, z) to (X, Y, Z) Coordinate Systems.

The relation between the polar coordinate systems referred to (x, y, z) and (X, Y, Z) is shown in Figure 8. The former is distinguished

from the latter by suffix 0, and evidently $\varphi=\varphi_0$. Solutions of wave equation expressed by means of $(r_0, \theta_0, \varphi_0)$ can be transformed to those referred to the system (r, θ, φ) through the relations [Onda and Sato (1969)]

$$\left.\begin{aligned} h_n^{(2)}(kr_0)\cdot P_n^m(\cos\theta_0) &= \sum_{l=0}^{\infty}\varepsilon_l^{n,m} j_{l+m}(kr)\cdot P_{l+m}^m(\cos\theta) \qquad b>r \\ &= \sum \zeta_l^{n,m} h_{l+m}^{(2)}(kr)\cdot P_{l+m}^m(\cos\theta) \qquad b<r \end{aligned}\right\} \quad (1\cdot5\cdot1)$$

where $\varepsilon_l^{n,m}$ have following expressions,

$$\left.\begin{aligned} &\varepsilon_l^{0,0}=(2l+1)\cdot h_l^{(2)}(kb) \\ &\varepsilon_l^{1,0}=(2l+1)\{l\cdot h_l^{(2)}(kb)/kb-h_{l+1}^{(2)}(kb)\} \\ &\varepsilon_l^{2,0}=\frac{3}{2}(2l+1)\left\{-\frac{2}{3}h_l^{(2)}(kb)+2\cdot h_{l+1}^{(2)}(kb)/kb+l(l-1)h_l^{(2)}(kb)/(kb)^2\right\} \\ &\varepsilon_l^{1,1}=(2l+3)\cdot h_{l+1}^{(2)}(kb)/kb \\ &\varepsilon_l^{2,1}=3(2l+3)\{l\cdot h_{l+1}^{(2)}(kb)/(kb)^2-h_{l+2}^{(2)}(kb)/kb\} \\ &\varepsilon_l^{2,2}=3(2l+5)\cdot h_{l+2}^{(2)}(kb)/(kb)^2 \end{aligned}\right\} \quad (1\cdot5\cdot2)$$

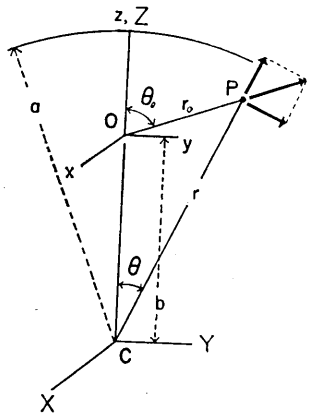

Fig. 8. Relation between coordinate systems (x, y, z) and (X, X, Y). The system (Y, Y, Z) is the same as that in Figure 7 and (x, y, z) the same as that in Figures 1, 2 and 4.

The function $\zeta_l^{n,m}$ can be obtained from $\varepsilon_l^{n,m}$ by replacing $h_{l+m}^{(2)}$ by j_{l+m}.

As to the transformation of coordinate system from (x, y, z) to (X, Y, Z), the following formula is known.

$$\begin{aligned} &\mathrm{rot}\{F, 0, 0\}_{r_0} \\ &\quad=\mathrm{rot}\{F\cdot\cos(\theta_0-\theta),\ F\cdot\sin(\theta_0-\theta), 0\}_r \\ &\quad=\mathrm{rot}\left\{\frac{F}{r_0}\cdot(r-b\cos\theta), \frac{F}{r_0}b\sin\theta, 0\right\}_r \\ &\quad=\mathrm{rot}\left\{\frac{F}{r_0}\cdot r, 0, 0\right\}_r \\ &\quad+\mathrm{rot}\left\{-\frac{F}{r_0}b\cos\theta, \frac{F}{r_0}b\sin\theta, 0\right\}_r \\ &\quad=\mathrm{rot}\left\{\frac{F}{r_0}\cdot r, 0, 0\right\}_r+\mathrm{rot}\left\{0, 0, -\frac{F\cdot b}{r_0}\right\}_X \end{aligned} \quad (1\cdot5\cdot3)$$

In this relation, suffixes r_0, r and X represent coordinate systems $(r_0, \theta_0, \varphi_0)$, (r, θ, φ) and (X, Y, Z) respectively. Vector potential $\{F\cdot r/r_0, 0, 0\}_r$ of the first term will be called "radially polarized vector potential" and that of the second term $\{0, 0, -F\cdot b/r_0\}_X$ "vertically polarized vector

potential." The former give rise to the $S2$ wave, while the latter both to the $S1$ and $S2$ waves.

The following formula [Usami et al. (1962)] is also useful for reducing potentials. Putting

$$\psi_{n,m}=h_n^{(2)}(kr)\cdot P_n^m(\cos\theta)\cdot\begin{matrix}\sin\\\cos\end{matrix} m\varphi$$

we have

$$\begin{aligned}&\mathrm{rot}\cdot\mathrm{rot}\{0,0,\psi_{n,m}\}_X\\&=k^2\Big[-\frac{n-m+1}{(2n+1)(n+1)}\cdot\mathrm{rot}\cdot\mathrm{rot}\Big\{-\frac{r}{k}\psi_{n+1,m},0,0\Big\}_r-\frac{n+m}{n(2n+1)}\\&\quad\cdot\mathrm{rot}\cdot\mathrm{rot}\Big\{-\frac{r}{k}\psi_{n-1,m},0,0\Big\}_r-\frac{1}{n(n+1)}\,\mathrm{rot}\Big\{-r\frac{\partial}{\partial\varphi}\psi_{n,m},0,0\Big\}_r\Big]\end{aligned}\qquad(1\cdot5\cdot4)$$

The third term corresponds to the so-called $S1$ wave and the first and the second ones to the $S2$ waves.

§ 1.6. Expressions of Potentials Referred to (X, Y, Z) Coordinate

Scalar and vector potentials referred to the coordinate system (x, y, z) fixed to the earthquake origin can now be transformed to those referred to the (X, Y, Z) coordinate system through the formulas obtained in the previous sections. In this section, however, formulas are given only for the outer sphere $r>b$. For the inner sphere $r<b$, similar formulas can be obtained by changing $\zeta_l^{n,m}$ to $\varepsilon_l^{n,m}$ and $h_l^{(2)}$ to j_l.

a) Single force

$$\left.\begin{aligned}&\Phi=\frac{-jF_A}{4\pi\rho V_P{}^2}e^{jpt}\cdot\Lambda(V_P)\\&\boldsymbol{B}=\frac{-jF_A}{4\pi\rho V_S{}^2}e^{jpt}[\mathrm{rot}\{r\Lambda(V_S),0,0\}_r+\mathrm{rot}\{0,0,-b\Lambda(V_S)\}_X]\\&\Lambda(V)=\cos\theta_0'\cdot\sum_{l=0}^{\infty}\zeta_l^{1,0}\cdot h_l^{(2)}(pr/V)\cdot P_l(\cos\theta)\\&\qquad+\sin\theta_0'\cdot\cos(\varphi-\gamma)\sum_{l=0}^{\infty}\zeta_l^{1,1}\cdot h_{l+1}^{(2)}(pr/V)\cdot P_{l+1}^1(\cos\theta)\end{aligned}\right\}\qquad(1\cdot6\cdot1)$$

b) Single couple

$$\left.\begin{aligned}&\Phi=\frac{-jpM_0}{4\pi\rho V_P{}^3}e^{jpt}\cdot\Lambda(V_P)\\&\boldsymbol{B}=\frac{-jpM_0}{8\pi\rho V_S{}^3}e^{jpt}[\mathrm{rot}\{r\Lambda(V_S),0,0\}_r+\mathrm{rot}\{0,0,-b\Lambda(V_S)\}_X]\end{aligned}\right\}$$

$$
\left.
\begin{aligned}
&+\frac{jM_0}{8\pi\rho V_S{}^2}e^{jpt}[\mathrm{rot}\cdot\mathrm{rot}\{r\Xi,\,0,\,0\}_r+\mathrm{rot}\cdot\mathrm{rot}\{0,\,0,\,-b\Xi\}_X]\\
\Lambda(V)=&\cos 2\phi_0'\Big\{\frac{1}{6}\cos\theta_0'\cdot\sin 2(\varphi-\gamma)\sum_{l=0}^{\infty}\zeta_l^{2,2}\cdot h_{l+2}^{(2)}(pr/V)\cdot P_{l+2}^2(\cos\theta)\\
&-\frac{1}{3}\sin\theta_0'\cdot\sin(\varphi-\gamma)\sum\zeta_l^{2,1}\cdot h_{l+1}^{(2)}(pr/V)\cdot P_{l+1}^1(\cos\theta)\Big\}\\
&+\sin 2\phi_0'\Big\{-\frac{1+\cos^2\theta_0'}{12}\cos 2(\varphi-\gamma)\sum\zeta_l^{2,2}\cdot h_{l+2}^{(2)}(pr/V)\cdot P_{l+2}^2(\cos\theta)\\
&+\frac{1}{6}\sin 2\theta_0'\cdot\cos(\varphi-\gamma)\sum\zeta_l^{2,1}\cdot h_{l+1}^{(2)}(pr/V)\cdot P_{l+1}^1(\cos\theta)\\
&-\frac{1}{2}\sin^2\theta_0'\sum\zeta_l^{2,0}\cdot h_l^{(2)}(pr/V)\cdot P_l(\cos\theta)\Big\}\\
\Xi=&\cos\theta_0'\sum\zeta_l^{1,0}\cdot h_l^{(2)}(pr/V_S)\cdot P_l(\cos\theta)\\
&+\sin\theta_0'\cdot\cos(\varphi-\gamma)\sum\zeta_l^{1,1}\cdot h_{l+1}^{(2)}(pr/V_S)\cdot P_{l+1}^1(\cos\theta)
\end{aligned}
\right\}
\qquad (1\cdot6\cdot2)
$$

c) Dip slip

$$
\left.
\begin{aligned}
\Phi=&\frac{jpM_0}{4\pi\rho V_P{}^3}e^{jpt}\Lambda(V_P)\\
\boldsymbol{B}=&\frac{jpM_0}{8\pi\rho V_S{}^3}e^{jpt}[\mathrm{rot}\,\{r\Lambda(V_S),\,0,\,0\}_r+\mathrm{rot}\,\{0,\,0,\,-b\Lambda(V_S)\}_X]\\
\Lambda(V)=&\frac{2}{3}\cos 2\delta\cdot\sin(\varphi-\gamma)\sum_{l=0}^{\infty}\zeta_l^{2,1}\cdot h_{l+1}^{(2)}(pr/V)\cdot P_{l+1}^1(\cos\theta)\\
&+\sin 2\delta\cdot\Big\{\sum\zeta_l^{2,0}\cdot h_l{}^2(pr/V)\cdot P_l(\cos\theta)+\frac{\cos 2(\varphi-\gamma)}{6}\sum\zeta_l^{2,2}\cdot h_{l+2}^{(2)}(pr/V)\\
&\cdot P_{l+2}^2(\cos\theta)\Big\}
\end{aligned}
\right\}
\qquad (1\cdot6\cdot3)
$$

d) Strike slip

The same as the dip slip case except

$$
\begin{aligned}
\Lambda(V)=&-\frac{\sin\delta}{3}\sin 2(\varphi-\gamma)\sum_{l=0}^{\infty}\zeta_l^{2,2}\cdot h_{l+2}^{(2)}(pr/V)\cdot P_{l+2}^2(\cos\theta)\\
&+\frac{2}{3}\cos\delta\cdot\cos(\varphi-\gamma)\sum\zeta_l^{2,1}\cdot h_{l+1}^{(2)}(pr/V)\cdot P_{l+1}^1(\cos\theta)
\end{aligned}
\qquad (1\cdot6\cdot4)
$$

C. Equivalent Source

§ 1.7 Equivalent Source Function

A point source of earthquake within a homogeneous elastic sphere produces the displacement and stress discontinuity on the concentric spherical surface on which the source is located. Thus the discontinuity, which will be called "equivalent source function", is equivalent to the original source, in the sense that the solutions obtained from the following two methods are the same.

(1) Transfer the source function to polar coordinate referred to the center of the sphere and solve the problem under the condition of free surface.

(2) Divide the sphere into two parts at the concentric surface on which the source is located. Assume suitable waves satisfying the equation of motion in both inner and outer parts and solve the problem under the conditions satisfying (a) vanishing of stress on the free surface and (b) discontinuity of displacement and stress on the source surface amounting to the value calculated from the source function.

For a radially heterogeneous elastic sphere, it is quite difficult to transfer the source function to the polar coordinate referred to the earth's center and to make satisfy the equation of motion. Therefore, in the present study, the second method will be adopted using the equivalent source function.

§ 1.8 Equivalent Source Function due to Various Kinds of Force Systems

In section 1.6, the scalar and vector potentials valid for the outer sphere $r>b$ are given. Those for the inner sphere $r<b$ have similar expressions and the difference of these two on the source surface gives rise to the discontinuities of displacement and stress, namely, the equivalent source functions. In order to calculate these, relations between the coefficients $\varepsilon_l^{n,m}$, $\zeta_l^{n,m}$ and the spherical Bessel functions such as

$$\zeta_l^{2,1}\cdot\dot{h}_{l+1}^{(2)}-\varepsilon_l^{2,1}\cdot\dot{j}_{l+1}=3(2l+3)j/k^3b^4 \qquad (1\cdot8\cdot1)$$

are employed. The dots $(\cdot)$ mean d/db and the argument of the spherical Bessel functions $h_l^{(2)}$ and j_l is assumed to be kb, k being either p/V_P or p/V_S. Here, the discontinuities of displacement and stress components on the source surface are defined as

$$\Delta D=\lim_{\varepsilon\to0}(D_{r=b+\varepsilon}-D_{r=b-\varepsilon}) \qquad (1\cdot8\cdot2)$$

The equivalent source functions are now readily calculated from equations

in section 1.6, in which material constants take values at the source surface $r=b$.

a) Single force

Summation of equivalent source functions derived from scalar potential and radially and vertically polarized vector potentials gives

$$\Delta u=\Delta v=w=0$$

$$\begin{Bmatrix}\widehat{\Delta rr}\\ \widehat{\Delta r\theta}\\ \widehat{\Delta r\varphi}\end{Bmatrix}=-\frac{F_A e^{jpt}}{4\pi b^2}\left[\begin{Bmatrix}\cos\theta_0'\sum(2l+1)P_l\\ 0\\ 0\end{Bmatrix}+\sin\theta_0'\begin{Bmatrix}0\\ \sum\frac{2l+1}{l(l+1)}\cos(\varphi-\varphi_0')\left(\dot{P}_l^1+\underline{\frac{P_l^1}{\sin\theta}}\right)\\ -\sum\frac{2l+1}{l(l+1)}\sin(\varphi-\varphi_0')\left(\underline{\frac{P_l^1}{\sin\theta}}+\dot{P}_l^1\right)\end{Bmatrix}\right] \tag{1·8·3}$$

Argument of the associated Legendre function P_n^m is $\cos\theta$ and dot $(\cdot)$ means $d/d\theta$. Underlined terms show $S1$ wave. The scalar potential contributes to the equivalent source function $\widehat{\Delta rr}$ and the vertically polarized vector potential to $\widehat{\Delta r\theta}$ and $\widehat{\Delta r\varphi}$.

b) Single couple

The sum of the equivalent source functions derived from the scalar and vector potentials are

$$\begin{Bmatrix}\Delta u\\ \Delta v\\ \Delta w\end{Bmatrix}=\frac{M_0\cdot C_3 e^{jpt}}{4\pi\rho b^2 V_P^2}\begin{Bmatrix}\sum(2l+1)P_l\\ 0\\ 0\end{Bmatrix}+\frac{M_0 e^{jpt}}{8\pi\mu b^2}\begin{Bmatrix}0\\ \sum\frac{2l+1}{l(l+1)}\left(3C_2+\sin\theta_0'\cdot\sin(\varphi-\varphi_0')\right)\cdot\left(\dot{P}_l^1+\underline{\frac{P_l^1}{\sin\theta}}\right)\\ \sum\frac{2l+1}{l(l+1)}\left(3\frac{\partial}{\partial\varphi}C_2+\sin\theta_0'\cdot\cos(\varphi-\varphi_0')\right)\cdot\left(\underline{\frac{P_l^1}{\sin\theta}}+\dot{P}_l^1\right)\end{Bmatrix}$$

$$\begin{Bmatrix} \widehat{\Delta rr} \\ \widehat{\Delta r\theta} \\ \widehat{\Delta r\varphi} \end{Bmatrix} = -\frac{M_0 e^{ipt}}{8\pi b^3} \left[\begin{Bmatrix} -\sum 2(2l+1)\frac{3\lambda+2\mu}{\lambda+2\mu} C_3 \cdot P_l & + 0 & + 0 \\ 0 & +\sum (2l+1)\frac{3\lambda+2\mu}{\lambda+2\mu} C_3 \cdot \dot{P}_l + 0 & \\ 0 & + 0 & +\sum (2l+1)\cos\theta_0' \cdot \dot{P}_l \end{Bmatrix} \right.$$

$$+ \begin{Bmatrix} -\sum 2 \sin\theta_0' \cdot \sin(\varphi-\varphi_0') \cdot P_l^1 & + 0 \\ 0 & +\sum \frac{2\sin\theta_0' \sin(\varphi-\varphi_0')}{l(l+1)} \left(\dot{P}_l^1 + \underline{\frac{P_l^1}{\sin\theta}} \right) \\ 0 & +\sum \frac{2\sin\theta_0' \sin(\varphi-\varphi_0')}{l(l+1)} \left(\underline{\frac{P_l^1}{\sin\theta}} + \dot{P}_l^1 \right) \end{Bmatrix}$$

$$\left. + \begin{Bmatrix} 0 \\ \sum \frac{6C_1}{l(l+1)} \left(\dot{P}_l^2 + \underline{\frac{2P_l^2}{\sin\theta}} \right) \\ \sum \frac{6 \cdot \partial C_1/\partial\varphi}{l(l+1)} \left(\underline{\frac{P_l^2}{\sin\theta}} + \frac{\dot{P}_l^2}{2} \right) \end{Bmatrix} \right]$$

$$C_1 = \frac{1}{6}\left(\cos 2\phi_0' \cdot \cos\theta_0' \cdot \sin 2(\varphi-\varphi_0') - \frac{\sin 2\phi_0'}{2}(1+\cos^2\theta_0') \cdot \cos 2(\varphi-\varphi_0') \right)$$

$$C_2 = \frac{1}{3}\left(-\cos 2\phi_0' \cdot \sin\theta_0' \cdot \sin(\varphi-\varphi_0') + \frac{\sin 2\phi_0'}{2} \cdot \sin 2\theta_0' \cdot \cos(\varphi-\varphi_0') \right)$$

$$C_3 = -\frac{\sin 2\phi_0'}{2} \cdot \sin^2\theta_0' \qquad (1\cdot 8\cdot 4)$$

Underlined terms mean $S1$ wave. Contributions of various kinds of potentials which remain after the summation are tabulated below.

Table 1.

Potential		Δu	Δv	Δw	$\Delta\widehat{rr}$	$\Delta\widehat{r\theta}$	$\Delta\widehat{r\varphi}$
Φ		0			0		
B (A)	Radially polarized					0	
	Vertically polarized		1	1		0,2	2
B (Ξ)	Radially polarized					1	0,1
	Vertically polarized		1	1	1	1	1

Numerals mean the azimuthal order number m and blank indicates no contribution. It must be noted that contributions from vector potential derived from Ξ in (1·6·2) characterize the single couple force and the function Ξ does not appear in any other force systems employed in the present paper. Vertically polarized vector potential contributes

to many more components of the equivalent source functions than the radially polarized one does.

c) Dip slip

The equivalent source functions are

$$\begin{Bmatrix} \Delta u \\ \Delta v \\ \Delta w \end{Bmatrix} = -\frac{M_0 C_2 e^{jpt}}{4\pi\rho V_P^2 b^2} \begin{Bmatrix} \sum (2l+1) P_l \\ 0 \\ 0 \end{Bmatrix} - \frac{3M_0 e^{jpt}}{8\pi\mu b^2} \begin{Bmatrix} 0 \\ \sum \frac{2l+1}{l(l+1)} C_1 \left(\dot{P}_l^1 + \frac{P_l^1}{\sin\theta} \right) \\ \sum \frac{2l+1}{l(l+1)} \frac{\partial C_1}{\partial \varphi} \left(\frac{P_l^1}{\sin\theta} + \dot{P}_l^1 \right) \end{Bmatrix}$$

$$\begin{Bmatrix} \widehat{\Delta rr} \\ \widehat{\Delta r\theta} \\ \widehat{\Delta r\varphi} \end{Bmatrix} = -\frac{M_0 C_2 e^{jpt}}{8\pi b^3} \begin{Bmatrix} \frac{3\lambda+2\mu}{\lambda+2\mu} \sum 2(2l+1) P_l + 0 \\ 0 \qquad\qquad -\frac{3\lambda+2\mu}{\lambda+2\mu} \sum (2l+1) \dot{P}_l \\ 0 \qquad\qquad + 0 \end{Bmatrix}$$

$$+ \frac{3M_0 e^{jpt}}{8\pi b^3} \begin{Bmatrix} 0 \\ \sum \frac{2(2l+1)}{l(l+1)} C_3 \left(\dot{P}_l^2 + \frac{2P_l^2}{\sin\theta} \right) \\ \sum \frac{2(2l+1)}{l(l+1)} \frac{\partial C_3}{\partial \varphi} \left(\frac{P_l^2}{\sin\theta} + \frac{\dot{P}_l^2}{2} \right) \end{Bmatrix} \qquad (1\cdot8\cdot5)$$

$$C_1 = \frac{2}{3} \cos 2\delta \cdot \sin(\varphi - \gamma), \quad C_2 = \sin 2\delta$$

$$C_3 = \frac{1}{6} \sin 2\delta \cdot \cos 2(\varphi - \gamma)$$

d) Strike slip

The equivalent source functions for the strike slip have the same expressions as the dip slip, except the constants C_1, C_2, C_3 which have the following expressions.

$$C_1 = \frac{2}{3} \cos\delta \cdot \cos(\varphi - \gamma)$$

$$C_2 = 0$$

$$C_3 = -\frac{\sin\delta}{3} \cdot \sin 2(\varphi - \gamma) \qquad (1\cdot8\cdot6)$$

It is noted that, for the strike slip, the equivalent source functions Δu and $\widehat{\Delta rr}$ become zero.

Table 2.

Potential		Δu	Δv	Δw	Δrr	$\Delta r\theta$	$\Delta r\varphi$
Φ		0			0	0	
B	Radially polarized					2	2
	Vertically polarized		1	1		2	2

For the cases of dip and strike slips, the contributions of vector and scalar potentials to the equivalent source functions are arranged in the Table 2. Here again, vertically polarized vector potential contributes to many more components of the equivalent source function than the radially polarized one does. Contribution from scalar potential Φ is confined to the case $m=0$, and they vanish for the strike slip, in other words, P wave does not contribute to the equivalent source function.

D. Method of Calculation of Theoretical Seismograms

§ 1.9 Basic Considerations

The equivalent source functions, namely, the amount of discontinuities of stress and displacement on the source surface calculated in the previous sections, can now be applied to the actual earth model, since the earth can be considered consisting of thin spherical homogeneous shells.

On the other hand, theoretical seismograms due to surface stress have been calculated by the present authors for various earth models from a simple homogeneous sphere [Usami and Satô (1964)] to a realistic model such as Gutenberg-Bullen A′ model [Satô and Usami (1970)]. The Common Spectrum, non-dimensional frequency and derivative of surface stress with respect to frequency $\partial E_S/\partial p$, $\partial E_T/\partial p$, $\partial E_t/\partial p$ were calculated. With the intention of using these numerical values, an attempt was made to reduce an internal source problem to a surface stress problem.

§ 1.10 Torsional Oscillation

In a radially heterogeneous earth model, let W be a function defining the radial distribution of displacement, then $E_t=\mu\left(\frac{dW}{dr}-\frac{W}{r}\right)$ gives radial distribution of stress components. Displacement and stress in the frequency domain are expressed by

$$\begin{Bmatrix} u(p) \\ v(p) \\ w(p) \end{Bmatrix} = \sum_{m,\,n} W_n(r) \cdot f^*(p) \begin{Bmatrix} 0 \\ \dfrac{mP_n^m(\cos\theta)}{\sin\theta} \cdot \begin{matrix} -\sin \\ \cos \end{matrix} m\varphi \\ -\dot{P}_n^m(\cos\theta) \cdot \begin{matrix} \cos \\ \sin \end{matrix} m\varphi \end{Bmatrix}$$

$$\begin{Bmatrix} \widehat{rr}(p) \\ \widehat{r\theta}(p) \\ \widehat{r\varphi}(p) \end{Bmatrix} = \sum_{m,\,n} E_t(r) \cdot f^*(p) \begin{Bmatrix} \\ \\ \\ \end{Bmatrix} \quad (1\cdot10\cdot1)$$

$f^*(p)$ is the Fourier transform of the time function of the applied force.

Then, distinguishing two solutions satisfying the equation

$$\mu\frac{d^2}{dr^2}W_n+\left(\frac{d\mu}{dr}+\frac{2\mu}{r}\right)\frac{dW_n}{dr}+\left(k^2\mu_a-\frac{1}{r}\frac{d\mu}{dr}-\frac{n(n+1)}{r^2}\right)W_n=0 \quad (1\cdot10\cdot2)$$

for a certain value of p by prefixes 1 and 2, we have [Satô et al. (1968)]

$$r^2[{}_1E_t\cdot{}_2W-{}_2E_t\cdot{}_1W]=\text{const.} \quad (1\cdot10\cdot3)$$

In order to find solutions for an internal source problem, we consider the following solutions of the equation of motion.

Table 3

Notation (prefix)	Condition on the surface		Amount of discontinuity at $r=b$		Remarks
	$E_t(a)$	$W(a)$	$E_t(b)$	$W(b)$	
$\bar{f}$	0	1	0	0	Free oscillation
$\bar{A}$			1	0	No disturbances within the source surface $r<b$
$\bar{B}$			0	1	
$\bar{I}$		1	0	0	Satisfy the condition at the center

Solutions satisfying the conditions of the free surface and of the stress discontinuity E_t amounting to $\delta_1\left(=\widehat{Ar\varphi}\cdot e^{-jpt}/\left(-\dot{P}_n^m\cdot\begin{matrix}\cos\\ \sin\end{matrix}m\varphi\right)\right)$ on the source surface $r=b$, can be expressed by the combination of solutions specified by prefixes $\bar{A}$ and $\bar{I}$.

$$W_{\delta 1}(r)=\delta_1({}_{\bar{A}}W(r)-{}_{\bar{A}}E_t(a)\cdot{}_{\bar{I}}W(r)/{}_{\bar{I}}E_t(a)) \quad (1\cdot10\cdot4)$$

Applying equation (1·10·3) to the solutions $\bar{f}$ and $\bar{A}$, we have

$$ {}_{\bar{A}}E_t(a)=\left(\frac{b}{a}\right)^2\cdot{}_{\bar{f}}W(b) \qquad (1\cdot10\cdot5) $$

Therefore

$$ W_{\delta 1}(r)=\delta_1\left({}_{\bar{A}}W(r)-\left(\frac{b}{a}\right)^2\cdot{}_{\bar{f}}W(b)\cdot{}_{\bar{I}}W(r)/{}_{\bar{I}}E_t(a)\right) \qquad (1\cdot10\cdot6) $$

Following a similar procedure, corresponding quantity due to the discontinuity of azimuthal displacement

$$ \delta_2\left(=\Delta w\cdot e^{-jpt}/(-\dot{P}_n^m\cdot\begin{matrix}\cos\\ \sin\end{matrix}m\varphi)\right) $$

is given by

$$ W_{\delta 2}(r)=\delta_2\left({}_{\bar{B}}W(r)+\left(\frac{b}{a}\right)^2\cdot{}_{\bar{f}}E_t(b)\cdot{}_{\bar{I}}W(r)/{}_{\bar{I}}E_t(a)\right) \qquad (1\cdot10\cdot7) $$

The solution in the time domain is obtained by the integral

$$ \begin{Bmatrix}v(t)\\ w(t)\end{Bmatrix}=\frac{1}{2\pi}\int_{-\infty}^{\infty}\begin{Bmatrix}v(p)\\ w(p)\end{Bmatrix}\cdot\exp(jpt)\cdot dp \qquad (1\cdot10\cdot8) $$

Putting (1·10·6) and (1·10·7) into (1·10·8), the quantities corresponding to the first terms of $W_{\delta 1}$ and $W_{\delta 2}$ become constant after the applied force becomes steady. For such a time range, the contributions from these terms are neglected since they are time-independent, the displacement being expressed by the sum of contributions from residues due to the second terms of $W_{\delta 1}$ and $W_{\delta 2}$.

Final expressions of displacement in the time domain are

$$ \begin{Bmatrix}u\\ v\\ w\end{Bmatrix}=-j\left(\frac{b}{a}\right)^2\sum_{m,\,n,\,i}\left[\frac{{}_{\bar{I}}W(r)}{\dfrac{\partial}{\partial p}{}_{\bar{f}}E_t(a)}(\delta_1\cdot{}_{\bar{f}}W(b)-\delta_2\cdot{}_{\bar{f}}E_t(b))\cdot f^*(p)\cdot\exp(jpt)\right]_{p={}_ip_n} $$

$$ \cdot\begin{Bmatrix}0\\ \dfrac{mP_n^m}{\sin\theta}\cdot\begin{matrix}-\sin\\ \cos\end{matrix}m\varphi\\ -\dot{P}_n^m\cdot\begin{matrix}\cos\\ \sin\end{matrix}m\varphi\end{Bmatrix} \qquad (1\cdot10\cdot9) $$

where δ_1 and δ_2 mean the equivalent source functions $\Delta\widehat{r\varphi}$ and Δw excluding the factors of the location (θ, φ) and time (t). At an eigenfrequency ${}_ip_n$, the root of $E_t(a)=0$, solution specified by prefix $\bar{I}$ is iden-

tical to that specified by $\bar{f}$. Numerical values of $\frac{\partial}{\partial p}{}_{\bar{I}}E(a)=\frac{\partial}{\partial p}{}_{\bar{J}}E(a)$, ${}_{\bar{J}}W(b)$ and ${}_{J}E_{t}(b)$ were given previously [Satô et al. (1968)]. Therefore, the displacement can now be calculated from the equation (1·10·9). Since the colatitudinal and azimuthal components have same radial distribution and they are accompanied by each other, it is enough to consider the equivalent source function either colatitudinal or azimuthal component.

§ 1.11. Spheroidal Oscillation

For a gravitating, radially heterogenous elastic sphere, solutions for the spheroidal oscillations in the frequency domain are

$$\left.\begin{aligned}\begin{Bmatrix}u(p)\\ v(p)\\ w(p)\\ \phi(p)\end{Bmatrix} &= \sum_{m,n} f^{*}(p) \begin{Bmatrix} U_n(r)\cdot P_n^m(\cos\theta)\cdot \begin{matrix}\cos\\ \sin\end{matrix} m\varphi \\ V_n(r)\cdot \dot{P}_n^m(\cos\theta)\cdot \begin{matrix}\cos\\ \sin\end{matrix} m\varphi \\ V_n(r)\cdot \dfrac{mP_n^m(\cos\theta)}{\sin\theta}\cdot \begin{matrix}-\sin\\ \cos\end{matrix} m\varphi \\ Y_n(r)\cdot P_n^m(\cos\theta)\cdot \begin{matrix}\cos\\ \sin\end{matrix} m\varphi \end{Bmatrix} \\ \begin{Bmatrix}\widehat{rr}(p)\\ \widehat{r\theta}(p)\\ \widehat{r\varphi}(p)\end{Bmatrix} &= \sum_{m,n} f^{*}(p) \begin{Bmatrix} E_S(r)\cdot P_n^m(\cos\theta)\cdot \begin{matrix}\cos\\ \sin\end{matrix} m\varphi \\ E_T(r)\cdot \dot{P}_n^m(\cos\theta)\cdot \begin{matrix}\cos\\ \sin\end{matrix} m\varphi \\ E_T(r)\cdot \dfrac{mP_n^m(\cos\theta)}{\sin\theta}\cdot \begin{matrix}-\sin\\ \cos\end{matrix} m\varphi \end{Bmatrix}\end{aligned}\right\} \qquad (1\cdot 11\cdot 1)$$

where U_n, V_n and Y_n are the radial distributions of radial and horizontal displacements and the gravity potential. From the differential equations for U_n, V_n, Y_n [Satô et al. (1967), equation (3.3)] a relation is found between two solutions for a certain value of frequency p, namely

$$r^2\Big[{}_2U\cdot{}_1E_S+n(n+1)\cdot{}_2V\cdot{}_1E_T-{}_1U\cdot{}_2E_S-n(n+1)\cdot{}_1V\cdot{}_2E_T + \frac{{}_2Y\cdot{}_1E_Y}{4\pi\Gamma}-\frac{{}_1Y\cdot{}_2E_Y}{4\pi\Gamma}\Big]=\text{const.} \qquad (1\cdot 11\cdot 2)$$

Prefixes 1 and 2 discriminate two solutions and Γ is the universal constant of gravity, n the colatitudinal order number and E_S, E_T, E_Y are defined as

$$\left.\begin{aligned} E_S &= (\lambda+2\mu)\dot{U}_n+\frac{2\lambda}{r}U_n-\frac{n(n+1)}{r}\lambda V_n \\ E_T &= \mu\Big(\dot{V}_n-\frac{V_n-U_n}{r}\Big) \\ E_Y &= \dot{Y}_n-4\pi\rho\Gamma U_n\end{aligned}\right\} \qquad (1\cdot 11\cdot 3)$$

E_S and E_T are the radial and horizontal stresses on the concentric spherical surface and E_Y the force on the same surface due to gravity potential. When the equivalent source function is given, solutions can be expressed by the combination of the following solutions.

Table 4

Notation (prefix)	Condition on the surface						Amount of discontinuity at $r=b$						Remarks
	E_S	E_T	E_q	U	V	Y	E_S	E_T	E_q	U	V	Y	
I	γ_1	0	0	1	α_1	β_1							Satisfy condition at the center
J	0	γ_2	0	1	α_2	β_2			0				
K	0	0	γ_3	1	α_3	β_3							
A							1	0	0	0	0	0	No disturbances within the source surface $r<b$
B							0	1	0	0	0	0	
C							0	0	0	1	0	0	
D							0	0	0	0	1	0	
f	0	0	0	1	0	0							No condition at the center
g	0	0	0	0	1	0			0				
k	0	0	0	0	0	1							

In this table

$$E_q=E_Y+\frac{n+1}{r}Y_n\,, \tag{1·11·4}$$

and

$$E_S(a)=E_T(a)=E_q(a)=0$$

gives the condition of the free spheroidal oscillation.

When the discontinuity E_S amounting to δ_3 is given on the source surface, the solution is expressed by the combination of solutions specified by prefixes I, J, K and A. From the condition of the free surface, we have

$$\left.\begin{aligned} I\cdot{}_IE_S+J\cdot{}_JE_S+K\cdot{}_KE_S+\delta_3\cdot{}_AE_S=0\\ I\cdot{}_IE_T+J\cdot{}_JE_T+K\cdot{}_KE_T+\delta_3\cdot{}_AE_T=0\\ I\cdot{}_IE_q+J\cdot{}_JE_q+K\cdot{}_KE_q+\delta_3\cdot{}_AE_q=0 \end{aligned}\right\} \tag{1·11·5}$$

Therefore, coefficients I, J and K are given by

$$\left.\begin{aligned} I&=-\delta_3\cdot{}_AE_S(a)/{}_IE_S(a)\\ J&=-\delta_3\cdot{}_AE_T(a)/{}_JE_T(a)\\ K&=-\delta_3\cdot{}_AE_q(a)/{}_KE_q(a) \end{aligned}\right\} \tag{1·11·6}$$

Using the relation (1·11·2) for the combinations of solutions (A, f), (A, g) and (A, k), we have

$$\left.\begin{aligned}
{}_AE_S(a)&=\left(\frac{b}{a}\right)^2\frac{{}_fU(b)}{{}_fU(a)}\cdot{}_AE_S(b)=\left(\frac{b}{a}\right)^2\cdot{}_fU(b)\\
{}_AE_T(a)&=\left(\frac{b}{a}\right)^2\frac{{}_gU(b)\cdot{}_AE_S(b)}{n(n+1)\cdot{}_gV(a)}=\left(\frac{b}{a}\right)^2\frac{{}_gU(b)}{n(n+1)}\\
{}_AE_q(a)&=4\pi\Gamma\left(\frac{b}{a}\right)^2\frac{{}_kU(b)\cdot{}_AE_S(b)}{{}_kY(a)}=4\pi\Gamma\left(\frac{b}{a}\right)^2\cdot{}_kU(b)
\end{aligned}\right\}\qquad(1\cdot11\cdot7)$$

Therefore, we have

$$U_{\delta3}(r)=\delta_3\cdot\left[{}_AU(r)-\left(\frac{b}{a}\right)^2\cdot\left(\frac{{}_fU(b)}{{}_IE_S(a)}\cdot{}_IU(r)+\frac{{}_gU(b)\cdot{}_JU(r)}{n(n+1){}_JE_T(a)}+\frac{4\pi\Gamma\cdot{}_kU(b)\cdot{}_KU(r)}{{}_KE_q(a)}\right)\right]\qquad(1\cdot11\cdot8)$$

$V(r)$ and $Y(r)$ have similar expressions.

When the equivalent source E_T, U and V amounting to δ_4, δ_5 and δ_6 respectively are given on the source surface, the function $U(r)$ are calculated following similar way. They are

$$\left.\begin{aligned}
U_{\delta4}(r)&=\delta_4\left[{}_BU(r)-\left(\frac{b}{a}\right)^2\cdot\left\{\frac{n(n+1){}_fV(b)}{{}_IE_S(a)}\cdot{}_IU(r)+{}_gV(b)\cdot\frac{{}_JU(r)}{{}_JE_T(a)}+4\pi\Gamma\cdot n(n+1)\cdot{}_kV(b)\cdot\frac{{}_KU(r)}{{}_KE_q(a)}\right\}\right]\\
U_{\delta5}(r)&=\delta_5\left[{}_CU(r)+\left(\frac{b}{a}\right)^2\cdot\left\{\frac{{}_fE_S(b)}{{}_IE_S(a)}\cdot{}_IU(r)+\frac{{}_gE_S(b)}{n(n+1)}\cdot\frac{{}_JU(r)}{{}_JE_T(a)}+4\pi\Gamma\cdot{}_kE_S(b)\cdot\frac{{}_KU(r)}{{}_KE_q(a)}\right\}\right]\\
U_{\delta6}(r)&=\delta_6\left[{}_DU(r)+\left(\frac{b}{a}\right)^2\cdot\left\{\frac{n(n+1){}_fE_T(b)}{{}_IE_S(a)}\cdot{}_IU(r)+{}_gE_T(b)\cdot\frac{{}_JU(r)}{{}_JE_T(a)}+4\pi\Gamma\cdot n(n+1)\cdot{}_kE_T(b)\cdot\frac{{}_KU(r)}{{}_KE_q(a)}\right\}\right]
\end{aligned}\right\}\qquad(1\cdot11\cdot9)$$

Displacement in the time domain is obtained by the integration of the form (1·10·8). Carrying out the integration, the first terms of equations (1·11·8) and (1·11·9) are found to be time-independent after the applied force becomes steady. These terms will be neglected in the numerical work.

Contributions from the other terms come from residues and we have

$$U_n(r)=-j\left(\frac{b}{a}\right)^2\left[\frac{{}_IU(r)}{\frac{\partial}{\partial p}{}_IE_S(a)}\left\{\delta_3\cdot{}_fU(b)+n(n+1)\delta_4\cdot{}_fV(b)\right.\right.$$

$$-\delta_5\cdot_f E_S(b)-n(n+1)\delta_6\cdot_f E_T(b)\Big\}$$
$$+\frac{{}_JU(r)}{\dfrac{\partial}{\partial p}{}_JE_T(a)}\left\{\frac{\delta_3\cdot_g U(b)}{n(n+1)}+\delta_4\cdot_g V(b)-\frac{\delta_5\cdot_g E_S(b)}{n(n+1)}-\delta_6\cdot_g E_T(b)\right\}$$
$$+\frac{4\pi\Gamma\cdot_K U(r)}{\dfrac{\partial}{\partial p}{}_KE_q(a)}\left\{\delta_3\cdot_k U(b)+n(n+1)\delta_4\cdot_k V(b)-\delta_5\cdot_k E_S(b)-n(n+1)\delta_6\cdot_k E_T(b)\right\}\Big] \tag{1·11·10}$$

Applying (1·11·2) to the combinations of solutions (I, J) and (J, K), we have, at $r=a$

$${}_JU\cdot_I E_S=n(n+1)\cdot_I V\cdot_J E_T,\qquad n(n+1)\cdot_K V\cdot_J E_T=\frac{{}_JY}{4\pi\Gamma}\cdot_K E_q \tag{1·11·11}$$

for arbitrary value of p. Therefore, when the frequency p approaches the eigenvalue ${}_ip_n$, we have

$$\frac{\partial}{\partial p}{}_IE_S(a)=n(n+1)\cdot\left(\frac{V}{U}\right)_{r=a}\cdot\frac{\partial}{\partial p}{}_JE_T(a)=\frac{1}{4\pi\Gamma}\left(\frac{Y}{U}\right)_{r=a}\cdot\frac{\partial}{\partial p}{}_KE_q(a) \tag{1·11·12}$$

It is also known that, at eigenfrequencies, solutions I, J and K mean free oscillations and

$$\begin{aligned}&\text{solution }(I)=\text{solution }(J)=\text{solution }(K)\\&\quad=\text{solution }(f)+\left(\frac{V}{U}\right)_{r=a}\cdot\text{solution }(g)+\left(\frac{Y}{U}\right)_{r=a}\cdot\text{solution }(k)\end{aligned} \tag{1·11·13}$$

Employing (1·11·12) and (1·11·13), we can simplify the equation (1·11·10) in the following way

$$U_n(r)=-j\left(\frac{b}{a}\right)^2\cdot\frac{{}_IU(r)}{\dfrac{\partial}{\partial p}{}_IE_S(a)}\cdot[\delta_3\cdot_I U(b)+n(n+1)\delta_4\cdot_I V(b)$$
$$-\delta_5\cdot_I E_S(b)-n(n+1)\delta_6\cdot_I E_T(b)] \tag{1·11·14}$$

Expressions for $V_n(r)$ and $Y_n(r)$ are obtained by changing U with argument r to corresponding quantities V and Y. Since the relation between the colatitudinal and azimuthal components for both displacement and stress in the expression (1·11·1) is similar to that in the equivalent source functions, it is sufficient to consider the colatitudinal component of equivalent source function of displacement and stress. Thus, the final form of displacement can be obtained as

$$\begin{Bmatrix} u(t) \\ v(t) \\ w(t) \end{Bmatrix} = -j\left(\frac{b}{a}\right)^2 \sum_{m,n,i} \left[\frac{f^*(p)\cdot\exp(jpt)}{\dfrac{\partial}{\partial p}{}_I E_S(a)} \right.$$

$$\left. \times \begin{pmatrix} \delta_3 \cdot {}_I U(b) + n(n+1)\delta_4 \cdot {}_I V(b) \\ -\delta_5 \cdot {}_I E_S(b) - n(n+1)\delta_6 \cdot {}_I E_T(b) \end{pmatrix} \right]_{p={}_i p_n} \begin{Bmatrix} {}_I U(r)\cdot P_n^m \cdot \begin{matrix}\cos\\ \sin\end{matrix} m\varphi \\ {}_I V(r)\cdot \dot{P}_n^m \cdot \begin{matrix}\cos\\ \sin\end{matrix} m\varphi \\ {}_I V(r)\cdot \dfrac{mP_n^m}{\sin\theta} \cdot \begin{matrix}-\sin\\ \cos\end{matrix} m\varphi \end{Bmatrix}$$

(1·11·15)

where δ_3, δ_4, δ_5 and δ_6 stand for the equivalent source functions $\widehat{\Delta rr}$, $\widehat{\Delta r\theta}$, Δu and Δv excluding factors relating to the time and the location on the surface.

Part II. Time Function of Applied Force and Theoretical Seismograms of Surface Waves with Special Reference to the Relation between Earthquake Energy and Magnitude

In Part II, theoretical seismograms of surface waves due to a buried source of normal dip slip fault are calculated using the equations (1·10·9) and (1·11·15). The results are affected by various kinds of parameters such as the type of fault, geometry, time function and depth of the source and location of observation point. Among these parameters, the effect of time function of applied force on surface waves will be investigated and special attention will be paid to the relation between earthquake energy and magnitude.

§ 2.1 Earth Model, Earthquake Source and Fundamental Properties of Free Oscillations

Gutenberg-Bullen A′ earth model [Usami et al. (1965)] was adopted. The radius of the earth is 6370 km and that of the core 3470 (=6370 −2900) km. The thickness of the crust is 32 km. P and S wave velocities in the crust are taken as 6.30 km/sec and 3.55 km/sec respectively. The focus, assumed to be in the crust, has 5.35 km depth. A double couple force associated with a normal dip slip fault of 60° dip angle is assumed to act at the focus. The line connecting the center and focus is taken as the z-axis and the direction of strike as $\varphi=0°$.

Several fundamental quantities necessary for computation and inter-

pretation of theoretical seismograms are shown in Figures 9, 10 and 11. Figure 9 shows the non-dimensional frequency $\eta=pa/V_{so}=(2\pi a/V_{so})/T$ of the spheroidal and torsional oscillations. V_{so} is the S wave velocity at the surface and T the period.

In the present study, only the surface waves are considered. Therefore, the fundamental modes ($i=1$) alone are employed. In Figure 9, the non-dimensional frequency for higher modes with $i=2\sim10$ are also shown. The largest value of η employed in the numerical computation is 2000, corresponding to $n=1970$ for torsional oscillation and to $n=2160$ for spheroidal mode. In other words, modes with period larger than about 5.5 sec are adopted. Curves in Figure 9 can be extended almost linearly to larger values of n. Non-dimensional frequency of spheroidal oscillation for smaller values of n is found in the former paper [Satô et al. (1967)].

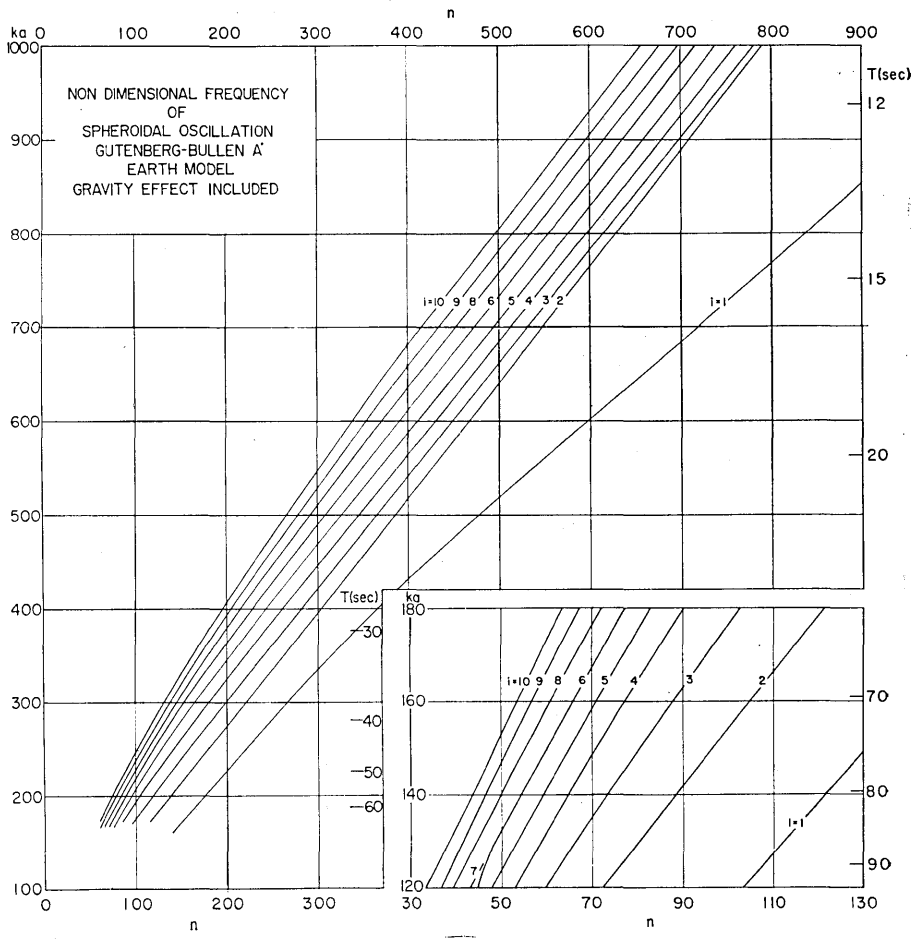

Fig. 9-a

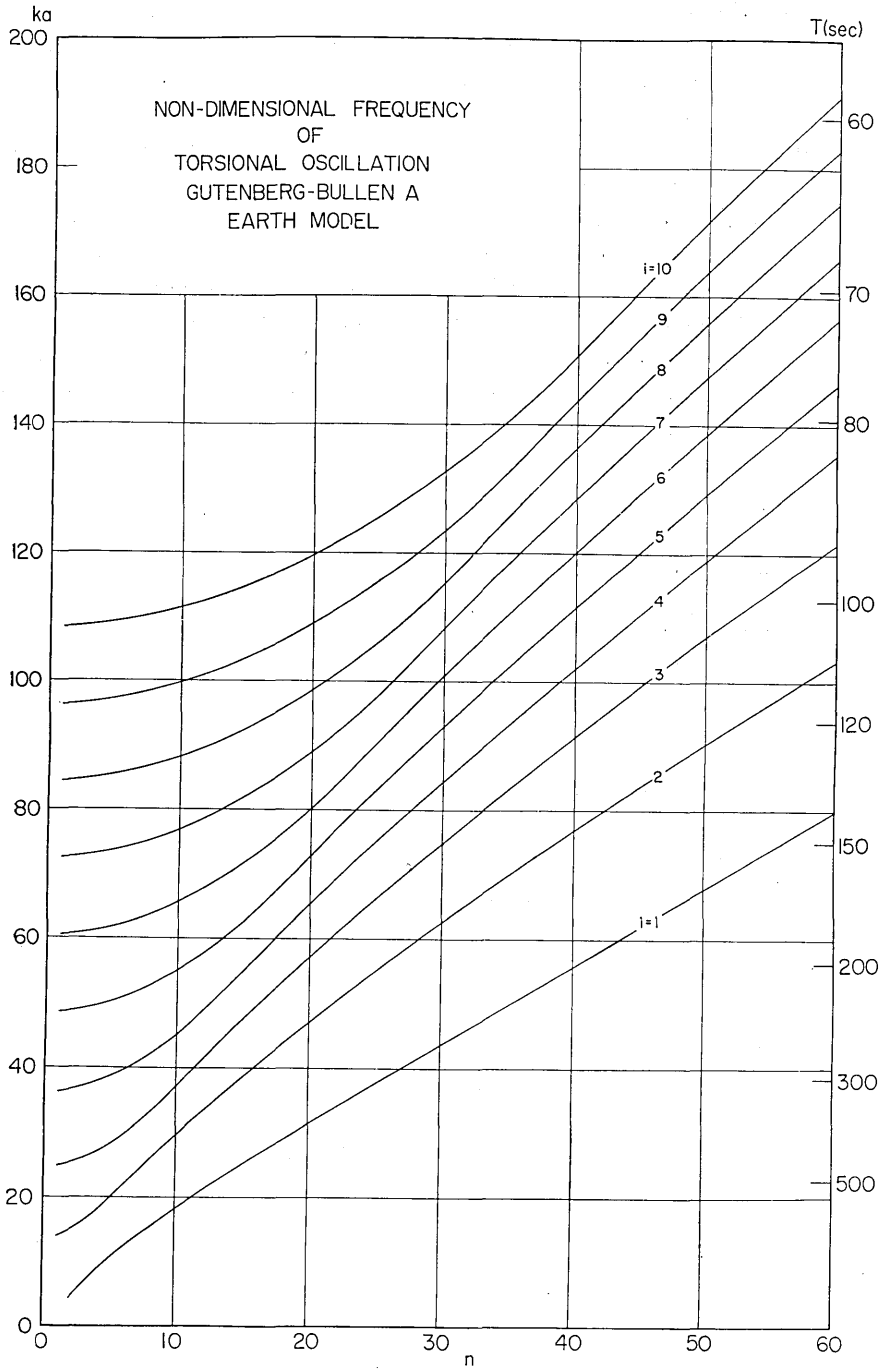
ka
T(sec)
NON-DIMENSIONAL FREQUENCY
OF
TORSIONAL OSCILLATION
GUTENBERG-BULLEN A
EARTH MODEL
i=10
9
8
7
6
5
4
3
2
i=1
200
180
160
140
120
100
80
60
40
20
0
60
70
80
100
120
150
200
300
500
0
10
20
30
40
50
60
n

Fig. 9-b

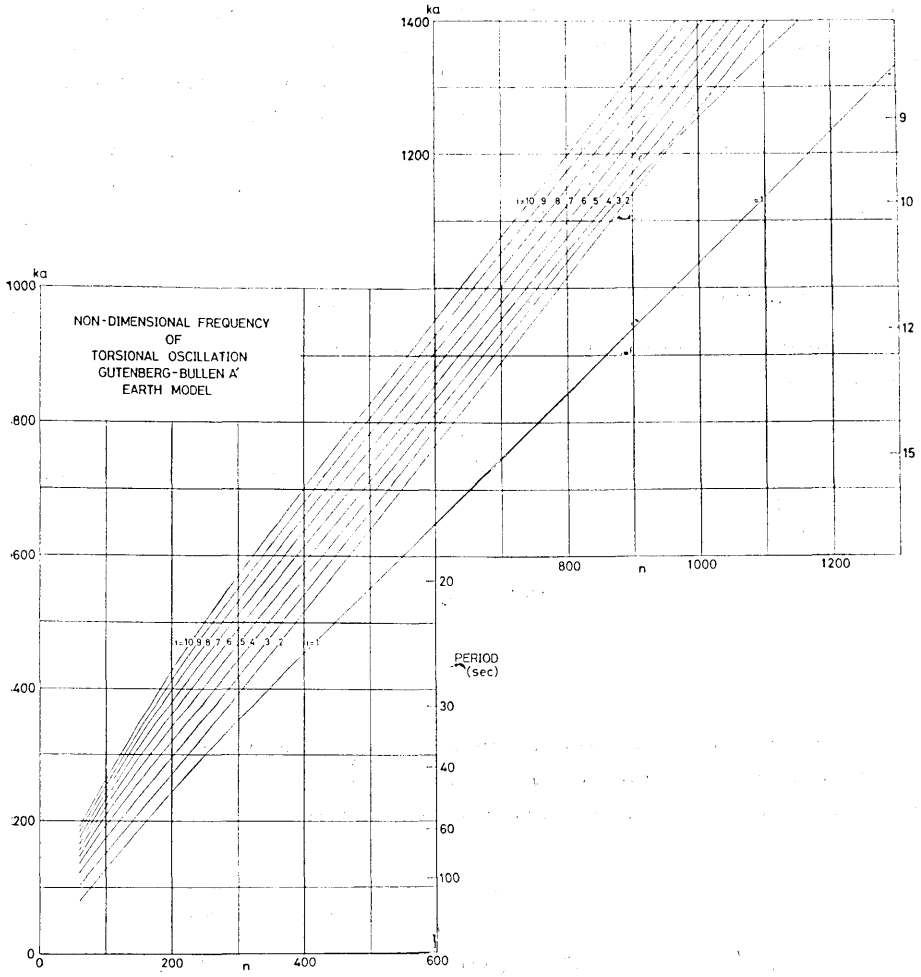

Fig. 9-c

Fig. 9. Non-dimensional frequency η of the spheroidal and torsional oscillations of Gutenberg-Bullen A′ earth model as function of colatitudinal order number n. $\eta=ka=(2\pi a/Vso)/T$, where a is the radius of the earth, Vso the S wave velocity on the surface and T the period. η of the spheroidal oscillation for smaller values of n is found in the former paper [Usami et al. (1965)]. Curves can be extended almost linearly to larger values of n.

Phase (C) and group (U) velocities of the spheroidal and torsional oscillations calculated from asymptotic formulas

$$\left.\begin{aligned} C/V_{so}&=\eta\Big/\left(n+\frac{1}{2}\right)\\ U/V_{so}&=d\eta/dn \end{aligned}\right\} \qquad (2\cdot1\cdot1)$$

are shown in Figures 10 and 11. The group velocity is important in inter-

preting surface waves and it is well known that the waves with the periods of maximum, minimum and flat group velocity appear predominantly on the seismograms. It should be remembered that in the present study the group velocity of the spheroidal oscillation has a maximum near period 60 sec and minimums near 18 sec and 220~230 sec and that of the torsional one is nearly flat for periods between 60 and 300 sec and has a minimum near 18 sec.

§ 2.2 Excitation Function and Time Function

Excitation functions for the spheroidal and torsional oscillations are defined as

$$\left.\begin{aligned} {}_i\mathscr{E}_n^S &= \frac{1}{\dfrac{\partial}{\partial p}{}_IE_S(a)}[\delta_3\cdot{}_IU(b)+n(n+1)\delta_4\cdot{}_IV(b)-\delta_5\cdot{}_IE_S(b)-n(n+1)\delta_6\cdot{}_IE_T(b)] \\ {}_i\mathscr{E}_n^T &= \frac{1}{\dfrac{\partial}{\partial p}{}_{\bar{I}}E_t(a)}[\delta_1\cdot{}_{\bar{J}}W(b)-\delta_2\cdot{}_{\bar{J}}E_t(b)] \end{aligned}\right\} \tag{2·2·1}$$

These are functions of the mechanism and focal depth of the source. Using the excitation function, the relations (1·11·15) and (1·10·9) giving the displacement on the surface are reduced to

$$\left.\begin{aligned} \begin{Bmatrix} u \\ v \\ w \end{Bmatrix} &= -j\left(\frac{b}{a}\right)^2 \sum_{m,n,i}[{}_i\mathscr{E}_n^S\cdot f^*(p)\cdot\exp(jpt)]_{p={}_ip_n}\begin{Bmatrix} U(a)\cdot P_n^m \overset{\cos}{\sin} m\varphi \\ V(a)\cdot \dot{P}_n^m \cdot \overset{\cos}{\sin} m\varphi \\ V(a)\cdot \dfrac{mP_n^m}{\sin\theta}\cdot \overset{-\sin}{\cos} m\varphi \end{Bmatrix} \\ \begin{Bmatrix} u \\ v \\ w \end{Bmatrix} &= -j\left(\frac{b}{a}\right)^2 \sum_{m,n,i}[{}_i\mathscr{E}_n^T f^*(p)\cdot\exp(jpt)]_{p={}_ip_n}\begin{Bmatrix} 0 \\ W(a)\cdot \dfrac{mP_n^m}{\sin\theta}\cdot \overset{-\sin}{\cos} m\varphi \\ -W(a)\cdot \dot{P}_n^m \cdot \overset{\cos}{\sin} m\varphi \end{Bmatrix} \end{aligned}\right\} \tag{2·2·2}$$

Common Spectrum defined in the previous papers [Satô et al. (1967, 1968)] is written as

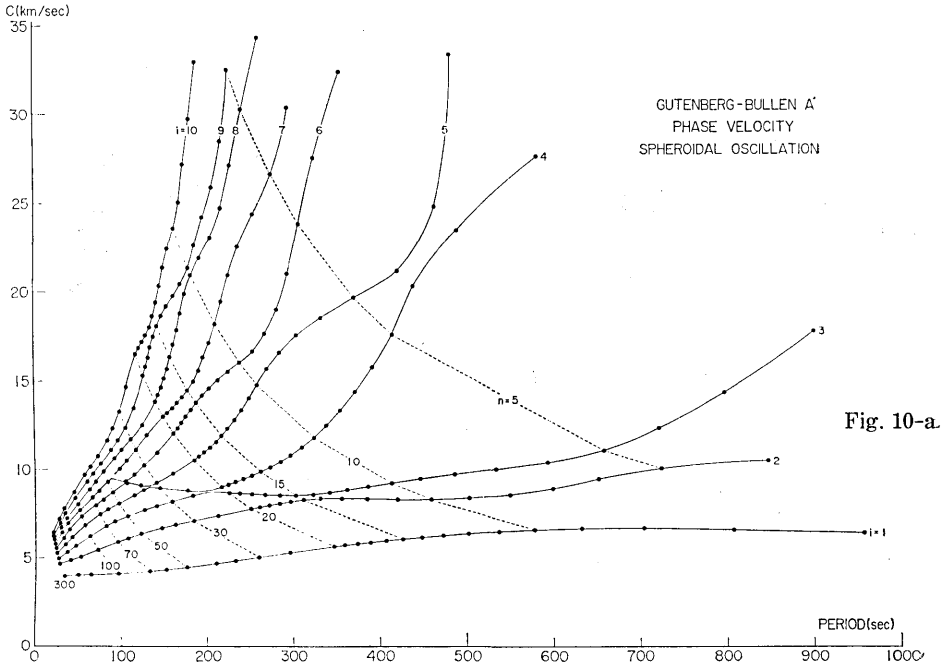

Fig. 10-a

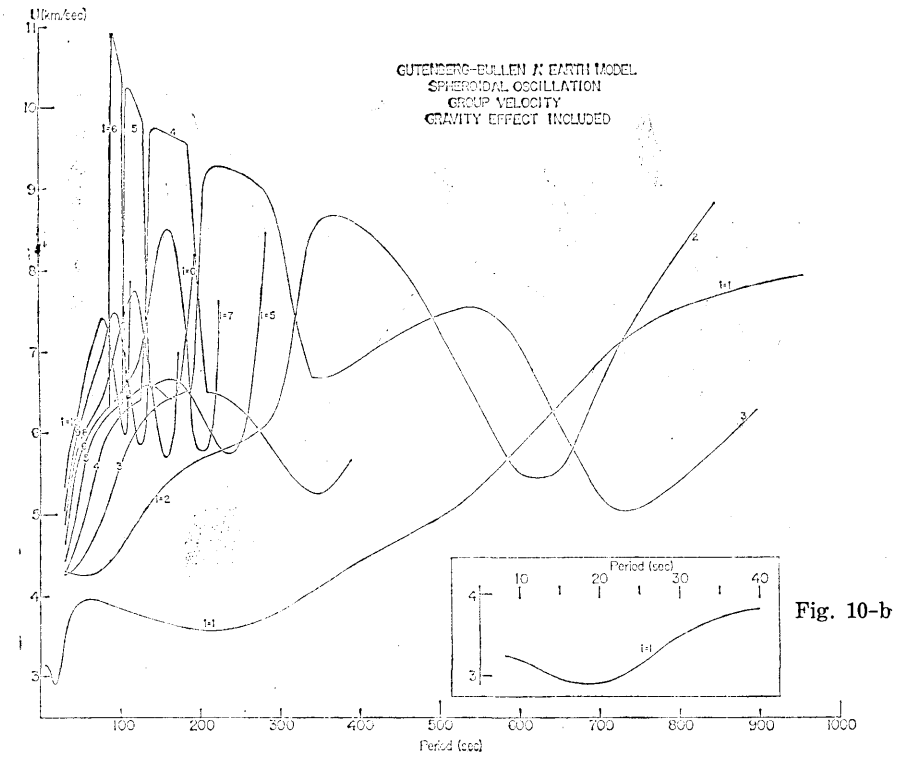

Fig. 10-b

Fig. 10. Phase and group velocities of the spheroidal oscillation as function of period.

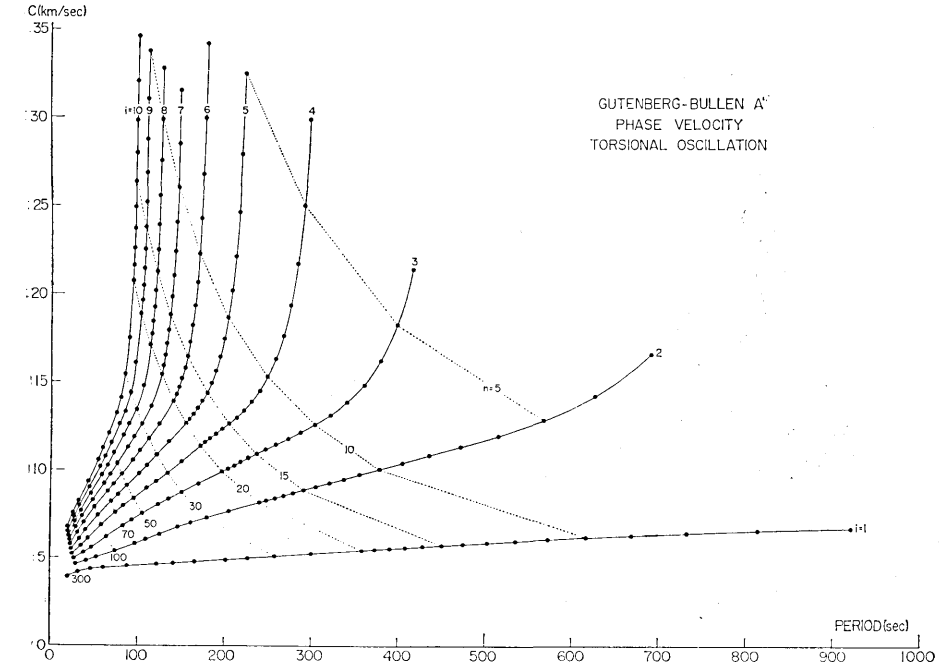

Fig. 11-a

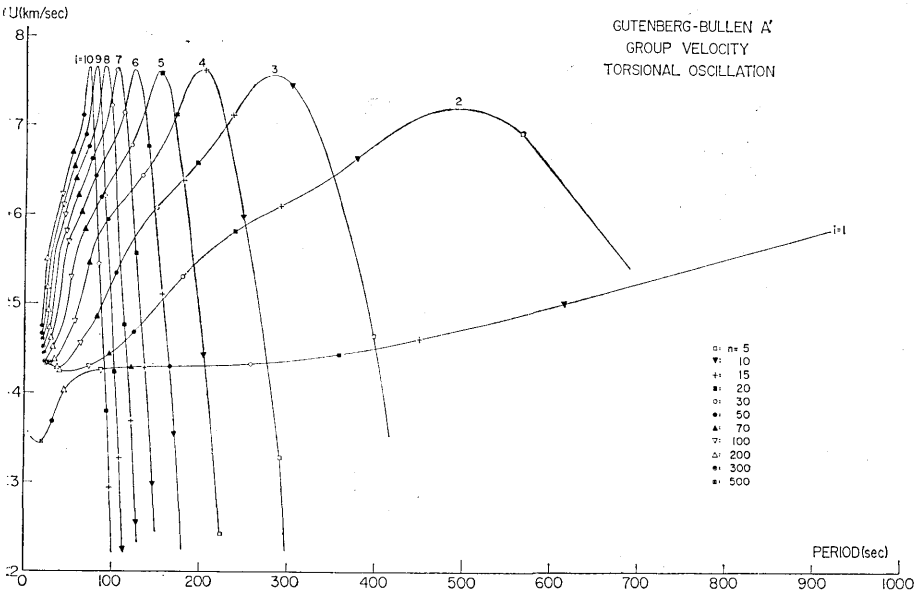

Fig. 11-b

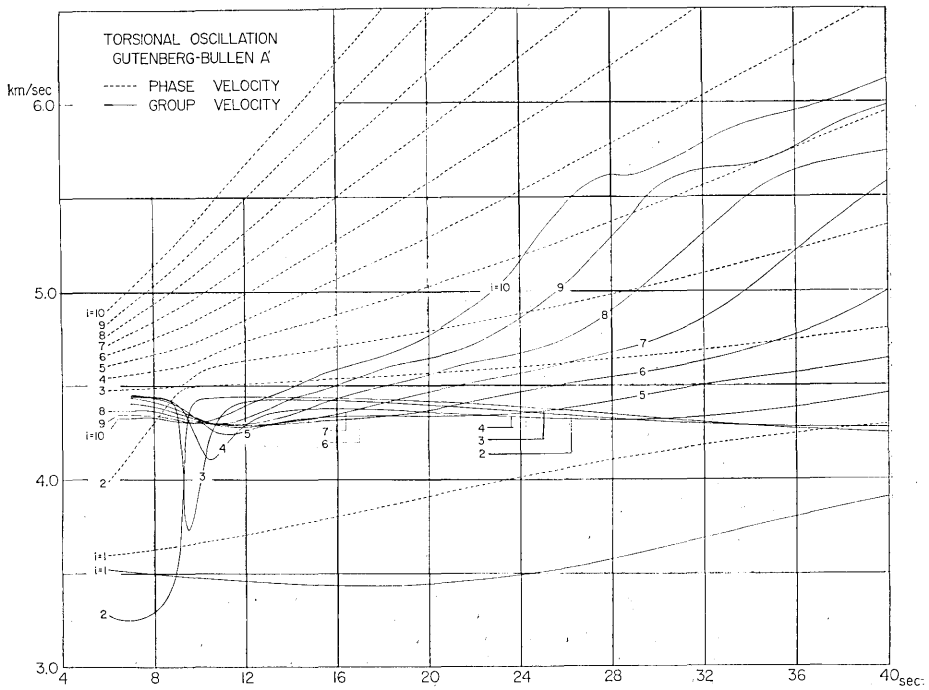

Fig. 11-c

Fig. 11. Phase and group velocities of the torsional oscillation as function of period.

$$\left.\begin{aligned} {}_iS_n^u &= {}_i\mathscr{E}_n^S \cdot f^*(p) \cdot U_n(a) \\ {}_iS_n^v &= {}_i\mathscr{E}_n^S \cdot f^*(p) \cdot V_n(a) \\ {}_iS_n^w &= {}_i\mathscr{E}_n^T \cdot f^*(p) \cdot W_n(a) \end{aligned}\right\} \qquad (2\cdot2\cdot3)$$

Common Spectrum is a function of external force and earth model, but does not depend on the time and the location of observation station and is conveniently used for the interpretation of the theoretical seismograms. However, in the present study, in order to save figure space, the excitation function and Fourier transform of the time function of applied force are drawn separately as functions of the colatitudinal order number n. In Figure 12, which shows the excitation function, the ordinate scale is rather complicated and has to be carefully read. For $m=0$ the excitation function of torsional mode vanishes for all values of n.

Time function, its Fourier transform and energy (cf. § 2.4) are given in Table 5. The unit of time is $2\pi a/V_{S0}=11267.6$ sec.

The time function of case 5 is invented in order to avoid infinite energy. It is composed of straight line and cosine functions and by controlling two parameters t_0 and t_1, we can make the time function as

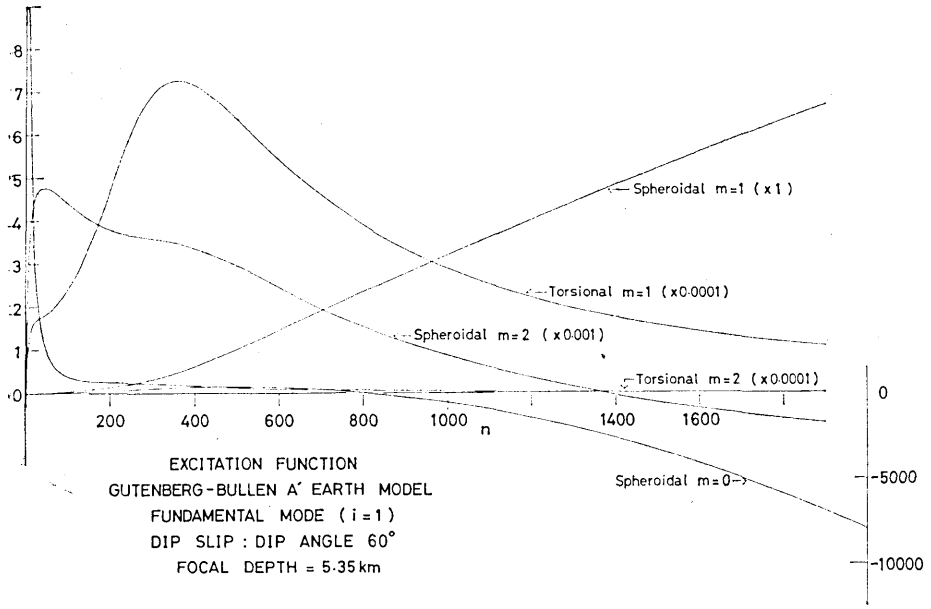

Fig. 12. Excitation function as function of colatitudinal order number n. For the torsional oscillation, it becomes zero when $m=0$. The ordinate scale on the right is for the spheroidal oscillation with $m=0$. For the other cases, the factor in the parenthesis has to be multiplied to the ordinate scale on the left. This large difference of magnitude comes from the fact that P_n^m is roughly the order of n^m when n is large.

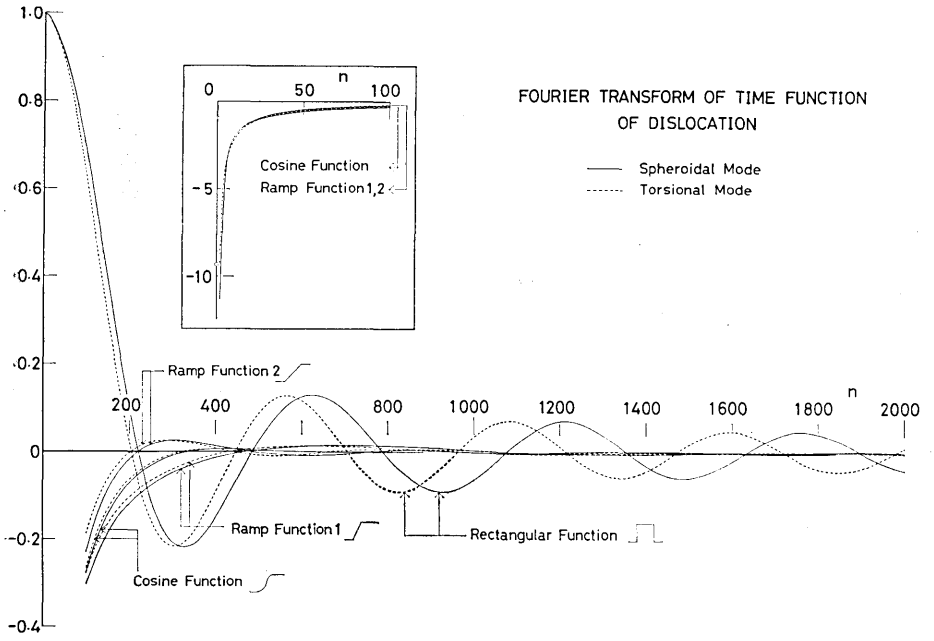

Fig. 13. Fourier spectrum of the time function for the cases given in Table 5. A factor (=250) is multiplied to all cases so that the values at $n=0$ become unity. Ramp function 1 and 2 correspond to the cases 3 and 4 of Table 5 respectively. Cases 3 and 5 show similar features and the discrepancy between them is too small to be expressed in the figure. Curves for the case 1 are omitted since they take the simple form of hyperbola $1/p$.

Table 5. Time function employed, its Fourier transform and energy.

Case	Name	Time function $f(t)$	Fourier transform $f^*(p)=\int_{-\infty}^{\infty} f(t)\cdot e^{-jpt}dt$	Energy		Remarks
				Expression*	Numerical value (10^{24}erg)	
1	Step function	$0 \quad t\leqq 0$ $1 \quad t>0$	$-j/p$	$(16/45)p_o^3$	2066.	
2	Rectangular function	$0 \quad \lvert t\rvert>t_o$ $1 \quad \lvert t\rvert\leqq t_o$ $(t_o=0.002)$	$2\sin(pt_o)/p$	$(32/15)\cdot[(p_o^3/3)$ $-(p_o^2/2t_o)\cdot\sin 2p_ot_o$ $-(p_o/2t_o^2)\cdot\cos 2p_ot_o$ $+(1/4t_o^3)\cdot\sin 2p_ot_o]$	4144.	
3	Ramp function	$0 \quad t\leqq 0$ $t/t_o \quad 0<t\leqq t_o$ $0 \quad t>t_o$ $(t_o=0.002)$	$-[2j\sin(pt_o/2)/p^2t_o]\cdot e^{-jpt_o/2}$	$(32/15)\cdot(1/t_o^2)\cdot(p_o-(1/t_o)\sin p_ot_o)$	29.3	
4	Same as above	〃 $(t_o=0.004)$	〃	〃	6.41	
5	Modified cosine ramp function	$0 \quad t\leqq 0$ $\alpha(1-\cos\beta t)/\beta \quad 0<t<t_1/2-t_o$ $1/2+\alpha(t-t_1/2) \quad t_1/2-t_o\leqq t\leqq t_1/2+t_o$ $1/2+\alpha t_o+(\alpha/\beta)\cdot\cos\beta(t-t_1) \quad t_1/2+t_o<t<t_1$ $1 \quad t_1\leqq t$ $(t_1=0.002,\ t_o=0.000975)$	$-[2j\alpha\beta^2/p(\beta^2-p^2)]\cdot[(\cos(pt_1/2)/\beta+(\sin pt_o)/p)]\cdot e^{-jpt_1/2}$	$\pi^3/(15(t_1/2-t_o)\cdot[t_o+(2/\pi)(t_1/2-t_o)]^2)$	367.	$\beta=\dfrac{\pi}{2\left(\frac{t_1}{2}-t_o\right)}$ $\alpha=\dfrac{1}{2\left(t_o+\frac{1}{\beta}\right)}$
6	Cosine ramp function	$0 \quad t\leqq 0$ $(1-\cos\pi t/t_o)/2 \quad 0<t\leqq t_o$ $1 \quad t_0<t$ $(t_o=0.004)$	$[j(\pi/t_o)^2/p(p^2-\pi^2/t_o^2)]\cdot\cos(pt_o/2)\cdot e^{-jpt_o/2}$	$(2/15)\cdot\pi^5/t_o^3$	2.71	

* unit$=\rho(M_o/4\pi\rho)^2(1/V_P{}^5+1.5/V_S{}^5)$

close to any of those of cases 1 and 3 as desired. The energy of case 5 is finite, which, therefore, can be used widely instead of step and ramp functions.

Fourier transform of the above time functions are given in Figure 13 as functions of n. In the figure, a normalization factor, which makes the total force of rectangular function unity, is multiplied for all cases.

§ 2.3 Theoretical Seismograms

Theoretical seismograms in the r-, θ-, and φ- directions were calculated at point $\theta=90°$, $\varphi=0°$ on the surface based on the equations $(1\cdot10\cdot9)$ and $(1\cdot11\cdot15)$ superposing only fundamental modes. Since contributions from the poles of the Fourier transform of $f(t)$ is usually time-independent after the applied force becomes steady, they are omitted in the synthesis work, which covers the time $t=0.195$ (0.00025) 0.330 including the passage of Rayleigh and Love waves. Calculated seismograms are shown in Figure 14. The unit of the ordinate scale is 0.176 cm when the moment of the double couple force is 10^{29} dyne-cm. Amplitudes of theoretical seismograms for the step and rectangular time functions are contracted in the ratio 1:10. Wave groups with periods 70, 30, 18, 13 and 9 sec. are clearly identified on the seismograms and their arrival times can be well explained by the group velocity. The radial displacement does not include torsional oscillation and in the azimuthal component the spheroidal oscillation is negligibly small compared to the torsional. The contributions of the spheroidal and torsional oscillations to the colatitudinal component is nearly the same.

It can be seen in the figure that the amplitudes of waves of about 70 sec period are nearly the same in all the cases notwithstanding the difference of the time function. Since the same amount of moment M_0 is assumed for all the cases, the above fact may indicate that the amplitude of long period surface wave is determined by the moment and not always by the time function of the applied force. On the other hand, shorter waves are much affected by the time functions and become larger as the degree of discontinuity of the time function increases.

§ 2.4 Energy of an Earthquake

Energy radiated in all directions from an earthquake source can be divided into two parts. The first part is the energy associated with the wave propagation and the second is the potential energy associated with permanent displacement. The former, integrated on the spherical surface of radius $\bar{r}$ surrounding the focus, is independent of $\bar{r}$, while the latter, integrated over the same spherical surface, diminishes as $\bar{r}$ in-

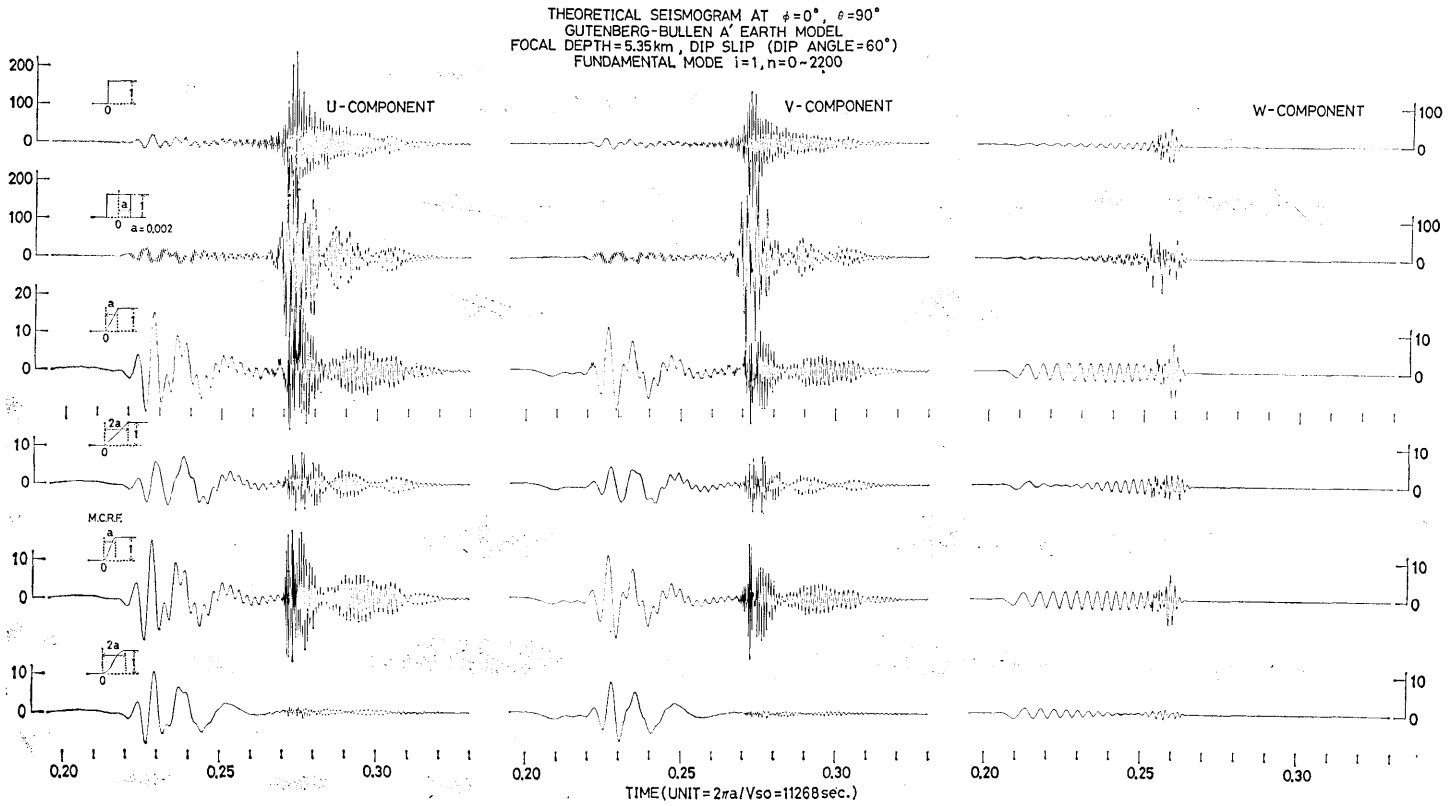

Fig. 14. Theoretical seismogram of disturbance at point ($\theta=90°$, $\varphi=0°$) on the surface of the earth due to a double couple force system associated with dip slip fault with 60° dip angle. Contributions from fundamental modes with order number $n=0\sim2200$ are summed up to represent surface (Rayleigh and Love) waves. $2\pi a/V_{SO}=11268$ seconds is taken as the unit of time. Ordinate scale is 0.176 cm when the moment of double couple force is 10^{29} dyne·cm. Seismograms, from up to down, correspond to cases 1, 2, ··· 6 of Table 5.

creases. In the present paper, the former quantity is defined as the energy of earthquake. It is expressed by

$$E=2(E_P+E_S) \tag{2·4·1}$$

and

$$E_{P,S}=\frac{1}{2}\int_0^{2\pi}d\varphi\int_0^{\pi}\sin\theta\cdot d\theta\int_{-\infty}^{\infty}\rho(\dot{u}^2+\dot{v}^2+\dot{w}^2)_{P,S}\cdot\bar{r}^2\cdot V_{P,S}\cdot dt \tag{2·4·2}$$

where dot $(\cdot)$ means d/dt and $\bar{r}$ is the radius of spherical surface on which the radiated energy is evaluated. On the right side of (2·4·1) the factor 2 comes from the fact that the kinetic and potential energy associated with wave propagation are the same. The following relation between the time function and its Fourier transform is well-known

$$\int_{-\infty}^{\infty}|f(t)|^2dt=\frac{1}{2\pi}\int_{-\infty}^{\infty}|f^*(p)|^2dp \tag{2·4·3}$$

By this formula, (2·4·2) is reduced to

$$E_{P,S}=\frac{1}{4\pi}\int d\varphi\int\sin\theta\cdot d\theta\int\rho(\hat{\dot{u}}^2+\hat{\dot{v}}^2+\hat{\dot{w}}^2)_{P,S}\cdot\bar{r}^2\cdot V_{P,S}\cdot dp \tag{2·4·4}$$

where $\hat{\dot{u}}$, $\hat{\dot{v}}$ and $\hat{\dot{w}}$ are Fourier transforms of $\dot{u}$, $\dot{v}$ and $\dot{w}$ respectively. In the expressions of particle velocity $\dot{u}$, $\dot{v}$ and $\dot{w}$, only the terms diminishing with the order of $1/r$ are adopted. Then, the v- and w- components of P wave and the u-component of S wave vanish. Referring to the equations (1·3·7) and (1·3·8), we obtain

$$\left.\begin{aligned}
\hat{\dot{u}}&=\frac{M_0}{4\pi\rho}p^2\cdot\frac{1}{r}f^*(p)\cdot\frac{1}{V_P^{\,3}}R_d\cdot\exp(-jpr/V_P)\\
\hat{\dot{v}}&=\quad\ \ \prime\prime\qquad\cdot\frac{1}{2V_S^{\,3}}\frac{\partial}{\partial\theta}R_d\cdot\exp(-jpr/V_S)\\
\hat{\dot{w}}&=\quad\ \ \prime\prime\qquad\cdot\frac{1}{2V_S^{\,3}}\frac{1}{\sin\theta}\cdot\frac{\partial}{\partial\varphi}R_d\cdot\exp(-jpr/V_S)
\end{aligned}\right\} \tag{2·4·5}$$

Employing the relation

$$\left.\begin{aligned}
&\int_0^{2\pi}d\varphi\int_0^{\pi}\sin\theta\cdot(R_d)^2d\theta=\frac{16}{15}\pi\\
&\int_0^{2\pi}d\varphi\int_0^{\pi}\sin\theta\cdot\left[\left(\frac{\partial}{\partial\theta}R_d\right)^2+\frac{1}{\sin^2\theta}\left(\frac{\partial}{\partial\varphi}R_d\right)^2\right]d\theta=\frac{96}{15}\pi
\end{aligned}\right\} \tag{2·4·6}$$

total energy radiated as P and S waves becomes

$$E=2(E_P+E_S)=\frac{8}{15}\rho\left(\frac{M_0}{4\pi\rho}\right)^2\left(\frac{1}{V_P^5}+\frac{3}{2V_S^5}\right)\int_{-\infty}^{\infty}p^4\cdot|f^*(p)|^2dp \qquad (2\cdot4\cdot7)$$

For cases 1~4, the integral of (2·4·7) diverges. Therefore, we replace the upper limit of integral ∞ by p_0 and consider this integral as the energy of earthquake. p_0 is the maximum frequency used in the calculation. For the other cases the integral $2\cdot\int_0^{p_0}$ gives a faithful representation of energy as far as the fraction of $2\cdot\int_{p_0}^{\infty}$ to $2\cdot\int_0^{\infty}$ is negligibly small.

§ 2.5 Energy, Moment and Magnitude of Earthquake

Figure 15 shows the relation between the energy defined in the previous section and apparent amplitude measured from the theoretical seismograms. However, in the case 5, the energy integral (2·4·7) decreases rapidly for the range $p>\beta$, while in the range $p<\beta$, it does not show rapid changes. The value of β in Table 5 is 6×10^4, which is 5 times larger than the value of maximum frequency employed in the numerical work. Therefore, some fraction of the calculated energy is considered as effective for this case and the points belonging to this case should be moved left by an amount corresponding to the ratio of effective energy to the total. On the other hand, Fourier transform of the time function for the cases 3 and 5 show negligibly small difference for the frequency range employed in numerical calculations. Therefore, the effective energy of case 5 can reasonably be considered equal to the case 3. In fact, theoretical seismograms of both cases show good coincidence in wave form and amplitude. Thus, in Figure 15, points of case 5 should be moved to the vertical line shown by the arrow of case 3.

Vertical amplitude with about 70 sec period (squares) is nearly constant, indicating that the amplitude of waves of this period is not directly related to energy. Vertical

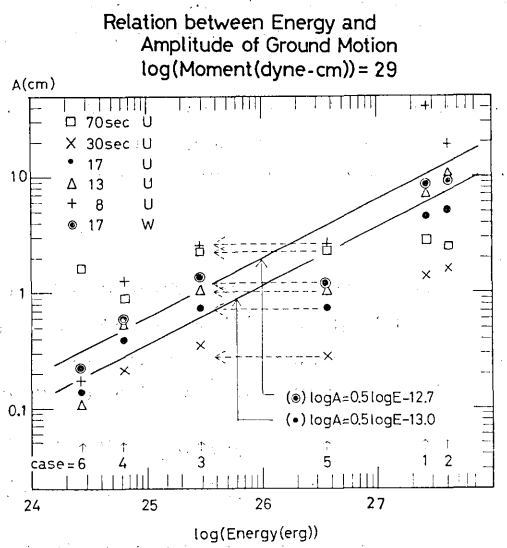

Fig. 15. Relation between energy of earthquake in Table 5 and amplitude of ground motion measured from the theoretical seismograms. Moment of double couple force is assumed to be 10^{29} dyne-cm. Case number corresponds to that in Table 5.

amplitude with 30 sec period (crosses $\times$) increase with energy at first, but the rate becomes small as the energy increases. This can be explained as follows. If we add modes with frequency larger than p_0, the energy increases rapidly, but the amplitude of waves with frequency smaller than p_0 does not increase so much. Therefore, as the energy increases, the curve of the amplitude as function of energy becomes flat.

For waves having shorter periods each kind of mark can be approximated by straight lines. Among such marks the groups of radial and azimuthal components of about 17 sec period are expressed as

$$\left.\begin{array}{ll} (1) & \log A(\mathrm{cm}) = 0.5 \log E(\mathrm{erg}) - 12.7 \quad (\mathrm{radial}) \\ (2) & \log A(\mathrm{cm}) = 0.5 \log E(\mathrm{erg}) - 13.0 \quad (\mathrm{azimuthal}) \end{array}\right\} \qquad (2\cdot5\cdot1)$$

From this relation, earthquake energy can be obtained from apparent amplitude of surface wave having 17 sec period. This statement premises implicitly that the ratio of energy shared by waves with 17 sec period to the total energy falls within a certain range. The equation (2·5·1) cannot be applied to earthquakes in which the above assumption of energy partition is not satisfied. In other words, for practical purposes, it is important to choose a suitable range of period which shares a nearly constant fraction of energy for a wide range of earthquake magnitudes. Period 20 sec might be a good choice for surface wave magnitude. In case 6, the energy fraction shared by shorter waves decreases more rapidly than the other cases as frequency increases. In fact, in Figure 15, points of this case for period shorter than 15 sec show much less amplitude than expected from the equation (2·5·1). Gutenberg (1945) defined surface wave mangnitude of an earthquake as

$$M = \log A + Q \qquad (2\cdot5\cdot2)$$

where A is the maximum ground amplitude of horizontal motion surface waves with period 20 sec expressed in microns and Q is a function of epicentral distance Δ. At $\Delta = 90°$, Q is 5.05. Using the definition of magnitude, we obtain from the equations (2·5·1).

$$\begin{array}{ll} (1) & \log E(\mathrm{erg}) = 2.0\,M + 7.32 \quad (\mathrm{radial}) \\ (2) & \log E(\mathrm{erg}) = 2.0\,M + 7.80 \quad (\mathrm{horizontal}) \end{array} \qquad (2\cdot5\cdot3)$$

Since the effect of force system, mechanism of earthquake source and azimuth of observation point are not considered, the numerical value of constant term in (2·5·3) may be subjected to future change. However, it must be noted that this constant takes a value 8 in the preliminary work using the result of Jeffreys [Richter (1958)]. In the

following, discussions will be limited to subjects not affected by the constant term of (2·5·3).

The coefficient, 2.0, of M in (2·5·3) means

$$E \propto A^2 \propto M_0^2, \tag{2·5·4}$$

which is also expected theoretically. Remembering that theoretical seismograms were calculated for different time functions assuming the same amount of moment M_0, we cannot but admit that, theoretically, the coefficient of M in the relation between $\log E$ and magnitude should be 2.0. On the other hand, widely adopted relation between magnitude and energy due to Richter (1958) is

$$\log E_G = 1.5\, M + 11.8 \tag{2·5·5}$$

in which the coefficient of M is 1.5 instead of 2.0.

The discrepancy of these two coefficients can be understood in the following way; namely the equations (2·5·3) and (2·5·5) express different kinds of energy. In fact, according to Gutenberg and Richter (1942) E_G means the energy conveyed by body wave with a period corresponding to maximum amplitude. However, the energy in equation (2·5·3) means total energy conveyed by all radiated waves having various periods. Executing the integral of the equation (2·4·7), it is easily recognized that

$$E \propto M_0^2 / t_r^3 \tag{2·5·6}$$

where t_r is a quantity having the dimension of time and can be considered as the process time for case 6. Another possible interpretation suggests that energy E_G is equal to energy expressed by (2·5·6). Assuming

$$M_0 \propto t_r^n$$

we have

$$E \propto t_r^{2n-3}, \qquad A \propto M_0 \propto t_r^n$$

and remembering that

$$\log E = 1.5\, M + 11.8 \quad \text{and} \quad M = \log A + Q$$

we obtain

$$n = 6\,,$$

that is

$$M_0 \propto t_r^6\,. \tag{2·5·7}$$

Among the two interpretations, the present authors would like to adopt the first one, that is, the standpoint that the energy E and E_G have different physical meanings.

§ 2.6 Simple Method of Estimating the Process Time

To estimate the process time at an earthquake origin is an important means of elucidating the secret of earthquake occurrance. As to this problem, the equation (2·5·7) suggests a simple method of estimating the process time of external force applied at the source. In fact, if we assume time function $f(t)$, process time can easily be calculated using the moment M_0 and energy E of an earthquake. For example, in the case 6 of Table 5

$$E=\frac{2\pi^5}{15}\left(\frac{M_0}{4\pi\rho}\right)^2\frac{1}{t_r^3}\rho\left(\frac{1}{V_P^5}+\frac{1.5}{V_S^5}\right) \qquad (2\cdot6\cdot1)$$

and E can be evaluated by

$$\log E=2.0\,M+7.80 \qquad (2\cdot6\cdot2)$$

Combining the two, t_r^3 is obtained from the known values.

Table 6 shows several examples.

Table 6

Location and date of earthquake	$\overline{M}_s$	S (10^4km^2)	M_0 (10^{29} dyne-cm)	E (10^{23}erg)	t_r (sec)
Alaska 1964 II 28	8.5	8	15	63	200 (3)
Aleutian 1965 II 4	7.75	5	5	2	440 (5)
Kurile 1963 X 13	8.25	2.5	1.5	20	67 (1)
Tokachi 1968 V 16	8.1	1.5	1.0	10	65 (1)
Kanto 1923 IX 1	8.2	1		16	

M_s: average of surface wave manitude, S: area of fault, M_0: moment, E: energy calculated by the second equation of (2 · 5 · 3), t_r: estimated process time assuming time function of case 6. Numerals in parenthesis are relative value of t_r.

Average values of surface wave magnitude $\overline{M}_s$ and moment M_0 were given by the courtesy of Dr. H. Kanamori (1970c). Since several assumptions are involved in this method, the authors do not insist that the value t_r in the table is numerically correct, however it is hoped that the relative time given in the parenthesis may give a key to interpret reasonably both magnitude $\overline{M}_s$ and moment M_0 which do not necessarily show good correlations for big earthquakes.

A more analytical and detailed method of estimating time process at a focus will be discussed in a future paper.

A part of the numerical computations was carried out at the Computer Centre of the University of Tokyo.

Glossary

a, b: radius of the earth and of source surface
A, B: vector potential of applied force and displacement
C, U: phase and group velocities
C_1, C_2, C_3: parameters defining force system as in (1·8·4)~(1·8·6)
E, E_G: earthquake energy defined in the present paper and by Gutenberg
E_S, E_T, E_Y, E_q, E_t: surface stresses defined in § 1.10 and (1·11·3), (1·11·4)
$f(t)$: time function of applied force
$f^*(p)$: Fourier transform of $f(t)$
F_A: magnitude of force
$F(t)$: defined in (1·2·2)
$\mathrm{F}(t)$, $\mathrm{F}_0(t)$: defined in (1·1·7) and (1·1·3)
$G(V)$: $F(t-r/V)/r$, V being the P or S wave velocity
H: defined in (1·2·4)
$h_l^{(2)}$, j_l: spherical Bessel functions
$\boldsymbol{I}(t)$: defined in (1·1·8)
i: radial mode number
j: unit of the imaginary number
k: p/V
K: external force distributed in volume
K_0: external force applied at a point
l: order of the spherical Bessel function
m: degree of the associated Legendre function $P_n^m(\cos\theta)$
n: order
M_0: moment of single or double couple force
M: earthquake magnitude
$P_n^m(\cos\theta)$: associated Legendre function by Ferrers' definition
p: angular frequency
R, r_0: see Fig. 1
R_1, R_d, R_s: defined in (1·2·10), (1·2·14) and (1·2·17)
(r, θ, φ): polar coordinate referred to the center of the earth
$(r_0, \theta_0, \varphi_0)$: polar coordinate referred to the source
${}_iS_n^u$, ${}_iS_n^v$, ${}_iS_n^w$: common spectrum of the radial, colatitudinal and azimuthal component
dS: see Fig. 1

$\widehat{rr}$, $\widehat{r\theta}$, $\widehat{r\varphi}$: stress component
t: time
T: period
t_r: process time
t_1, t_0: constant used in case 5 of Table 5
U: displacement
u, v, w: displacement component in the r-, θ- and φ-directions
$\dot{u}$, $\dot{v}$, $\dot{w}$: particle velocity in the r-, θ- and φ-component
$\hat{\dot{u}}$, $\hat{\dot{v}}$, $\hat{\dot{w}}$: Fourier spectrum of $\dot{u}$, $\dot{v}$, $\dot{w}$
U_n, V_n, W_n, Y_n: function giving radial distribution of displacement component and the gravity potential
V_P, V_S, V_{SO}: velocity of P and S waves and S wave velocity on the surface
v': volume in which all the external force is applied (see Fig. 1)
α, β: constants used in case 5 of Table 5
γ: strike direction of a fault
Γ: universal constant of gravity
δ: dip angle of a fault
δ_1, $\cdots$, δ_6: equivalent source function excluding factors related to the time and location
Δ: epicentral distance
$\varepsilon_l^{n,m}$, $\zeta_l^{n,m}$: coefficients defined in (1·5·1)
${}_i\mathscr{E}_n^S$, ${}_i\mathscr{E}_n^T$: excitation function of spheroidal and torsional oscillations
η: non-dimensional frequency $(=(2\pi a/V_{SO})/T)$
Θ, Φ: location of observation point referred to the polar coordinate (X, Y, Z). See Fig. 7
θ_s, φ_s: colatitude and longitude of observation point
θ_e, φ_e: colatitude and longitude of source
(θ_0', φ_0') direction of single force (see Fig. 2)
Λ, $\bar{\Lambda}$: quantity defined in § 1.3-(c)
λ, μ: Lamè's constant
Ξ: defined in (1·6·2)
ρ: density
ϕ, Φ: scalar potential of applied force and displacement
$\boldsymbol{\psi}$, $\boldsymbol{\Psi}$: vector potential of applied force and displacement
Ψ_e, Ψ_s: azimuth of the source and station as seen from the station and source
$\Psi_{n,m}$: solution of the equation of motion in polar coordinate
ϕ: gravitational potential due to disturbance

References

CHANDER, R., L. E. ALSOP and J. OLIVER, 1968, On the Synthesis of Shear-Coupled PL Waves, *Bull. Seism. Soc. Amer.*, **58**, 1849-1877.

GUTENBERG, B. and C. F. RICHTER, 1942, Earthquake Magnitude, Intensity, Energy, and Acceleration, *Bull. Seism. Soc. Amer.*, **32**, 163-192.

GUTENBERG, B., 1945, Amplitudes of Surface Waves and Magnitudes of Shallow Earthquakes, *Bull. Seism. Soc. Amer.*, **35**, 3-12.

KANAMORI, H., 1970a, Synthesis of Long-Period Surface Waves and its Application to Earthquake Source Studies—Kurile Island Earthquake of October 13, 1963—, *Jour. Geophys. Res.*, **75**, No. 26.

KANAMORI, H., 1970b, The Alaska Earthquake of 1964—Radiation of Long-Period Surface Waves and Source Mechanism—, *Jour. Geophys. Res.*, **75**, No. 26.

KANAMORI, H., 1970c, personal communication.

KEILIS-BOROK, V. I., 1950, Concerning the Determination of the Dynamic Parameters of a Focus, *Trudy Geofiz. In-ta AN SSSR*, No. 9.

LOVE, A. E. H., 1934, *A Treatise on the Mathematical Theory of Elasticity*, 4th ed., Cambridge Univ. Press.

ONDA, I. and R. SATO, 1969, Transformation of an Elastic Wave Solution related to Translation of the Origin of the Polar Coordinate System, *Bull. Earthq. Res. Inst.*, **47**, 599-611.

RICHTER, C. F., 1958, *Elementary Seismology*, Freeman and Company, 365-366.

SAITO, M., 1967, Excitation of Free Oscillations and Surface Waves by a Point Source in a Vertically Heterogeneous Earth, *Jour. Geophys. Res.*, **72**, 3689-3699.

SATO, R, 1969, Formulation of Solutions for Earthquake Source Models and Some Related Problems, *J. Phys. of the Earth*, **17**, 101-110.

SATÔ, Y., T. USAMI and M. EWING, 1962, Basic Study on the Oscillation of a Homogeneous Elastic Sphere IV, *Geophys. Mag.*, **31**, 237-242.

SATÔ, Y., T. USAMI and M. LANDISMAN, 1967, Theoretical Seismograms of Spheroidal Type on the Surface of a Gravitating Elastic Sphere. II. Case of Gutenberg-Bullen A' Earth Model, *Bull. Earthq. Res. Inst.* **45**, 601-624.

SATÔ, Y., T. USAMI and M. LANDISMAN, 1968, Theoretical Seismograms of Torsional Disturbances Excited at a Focus within a Heterogeneous Spherical Earth—Case of a Gutenberg-Bullen A' Earth Model, *Bull. Seism. Soc. Amer.*, **58**, 133-170.

SATÔ, Y. and T. USAMI, 1970, Theoretical Seismograms of Spheroidal Type on the Surface of a Gravitating Elastic Sphere. V. Case of Gutenberg-Bullen A' Earth Model (continued), *Bull. Earthq. Res. Inst.*, **48**, 521-531.

SINGH, S. J. and A. BEN-MENAHEM, 1969a, Eigenvibration of the Earth Excited by Finite Dislocations-I Toroidal Oscillations, *Geophys. J.*, **17**, 151-177.

SINGH, S. J. and A. BEN-MENAHEM, 1969b, Eigenvibrations of the Earth Excited by Finite Dislocations-II Spheroidal Oscillations, *Geophys. J.*, **17**, 333-350.

USAMI, T., K. KANO and Y. SATÔ, 1962, Some Remarks on the Solutions of the Equation of Motion for a Homogeneous and Isotropic Elastic Medium (II), *Geophys. Mag.*, **31**, 623-682.

USAMI, T. and Y. SATÔ, 1964, Propagation of Spherodial Disturbances on a Homogeneous Elastic Sphere, *Bull. Earthq. Res. Inst.*, **42**, 273-287.

USAMI, T., Y. SATÔ and M. LANDISMAN, 1965, Theoretical Seismograms of Spheroidal Type on the Surface of a Heterogeneous Spherical Earth, *Bull. Earthq. Res. Inst.*, **43**, 641-660.

USAMI, T., Y. SATÔ, M. LANDISMAN and T. ODAKA, 1968, Theoretical Seismograms on the Surface of a Gravitating Elastic Sphere III. Case of a Homogeneous Mantle with a Liquid Core, *Bull. Earthq. Res. Inst.*, **46**, 791-819.

USAMI, T. and Y. SATÔ, 1970, Theoretical Seismograms of Spheroidal Type on the Surface of a Gravitating Elastic Sphere. IV. Homogeneous Mantle with a Liquid Core Excited by Colatitudinal Force, *Bull. Earthq. Res. Inst.*, **48**, 351-362.

30. 理論地震記象と震源模型

(I) 理論

(II) 震源力の時間関数と表面波

地震研究所 宇佐美 龍 夫
東京大学大学院 小 高 俊 一
地震研究所 佐 藤 泰 夫

筆者らは地表面及び地下の球面上に働く力による弾性球面上の擾乱をいろいろなモデルについて計算し，理論地震記象の基本的な性質を明らかにすると同時に，その有用性を確かめてきた．この一連の論文は，実際の地震に際して震源に推定される力を地下のある深さの所に加えた場合の理論地震記象を取扱い震源模型と弾性波伝播との関係を明かにすることを目的とする．地球モデルとしては，グーテンベルグ・ブレン A' を採用する．

(I) 理　　論

弾性球内に働く力系による擾乱を求める式は斎藤・Singh and Ben-Menahem・佐藤 (良) などによって求められている．

筆者らは既にグーテンベルグ・ブレン A' モデルについていろいろな量の数値を持っている．これを有効に使うためには，上記の人々による式を書き替えなければならないが，それは必ずしも容易でないので，独立に理論式を作った．その考え方は次の通りである．

1. 等方等質弾性体を仮定し震源を原点とする座標系を使い，震源に働く力による媒質内の変位の表現式を作る．(I 章の A)
2. これを地球の中心を原点とする座標系に変換する．(I 章の B)
3. この表現式は震源のある同心球面の内側と外側では異なり，一般に震源球面上で変位及び歪力に不連続が現われる．これを "Equivalent Source Function" と名づける．(I 章の C)
4. 考える地球モデルの運動方程式を a. 自由表面の条件，b. 震源面での "Equivalent Source Function" を満足するように解いて解を得る．(I 章の D)

この様な手続中に，数値計算に便利な (1・11・12) 式が証明された．

(II) 震源力の時間関数と表面波

上記で求めた式の応用として，まず震源力の時間関数が表面波の伝播に及ぼす影響をしらべた．

1. 震源模型．傾斜角 60° の Dip Slip 型正断層と等値の複双力源を考える．震源の深さは，5.35 km．点震源とし，モーメント (M_0) の大きさを単位とするが後の議論では，$M_0=10^{29}$ dyne・cm とした．震源の方向を Z 軸とし，断層の走行の方向を経度 0° とした．
2. 地球の模型．グーテンベルグ・ブレン A' を採用した．地殻の厚さは 32km，地殻内の P 波，S 波の速度はそれぞれ 6.30 km/sec，3.55 km/sec である．
3. 理論地震記象．地表面上の 1 点 ($\theta=90°$，$\varphi=0°$) での理論地震記象を $t=0.195$ (0.00025) 0.330 について計算した．時間の単位は (地球の周長)/(表面での S 波速度)=11268 秒であるから実際には 2.8 sec おきに変位を計算したことになる．上記の時間は表面波の通過する時間を含んでいる．擾乱の計算には基準モード ($i=1$) のみを用い，無次元化された周波数 $\eta=(2\pi a/Vso)/T$ が 2000 以下のモードを加えた．
4. 無次元化した周波数，それから簡単に求められる位相速度及群速度，励起関数 (ε) と震源力の時間関数のフーリエ変換 $f^*(p)$ を図示した．とくに群速度では極大極小が現われ，周期 17～18 秒ではスフェロイド型，捩れ型の両振動に極小が認められる．励起関数 (ε) と従来使って来たコモン・スペクトラム (S) とは次の関係にある．

$$
\begin{aligned}
{}_iS_n{}^u &= {}_i\varepsilon_n{}^S \cdot f^*(p) \cdot U_n(a) \\
{}_iS_n{}^v &= {}_i\varepsilon_n{}^S \cdot f^*(p) \cdot V_n(a) \\
{}_iS_n{}^w &= {}_i\varepsilon_n{}^T \cdot f^*(p) \cdot W_n(a)
\end{aligned}
$$

5. 震源力の時間関数としては第 5 表にある 6 種のものを採用した．このうちの 5 番目のものは，6 番目と 3，4 番目の中間的なもので，直線と cos 関数をスムースにつなげたものである．エネルギーが有限になるし，二つの媒介変数を選ぶことにより，1，3，4，6 の何れにも移行出来て便利である．
6. 第 14 図にはこうして計算した理論地震記象が示されている．これによると長周期 (T=約 70 秒) の波の振幅は時間関数によらない．一方，短周期の波の振幅は時間関数の不連続性と共に増大する．この記象の走時や分散は群速度からよく説明できる．実際には，u- 成分はスフェロイド型振動のみ，w- 成分は捩り型のみと考えてよく，v- 成分は両者が混り合っている．
7. 地震のエネルギーとして震源から弾性波として放射されるものをとることにする．これは全振動エネルギーのうちから永久変位として残るポテンシャルエネルギーを除いたものと等しい．このエネルギーは，第 5 表の 1～4 では発散するので，この場合には実際に計算に使用したモードによるエネルギー和を求め，これをこの場合の理論地震記象に対するエネルギーと考えた．
8. このエネルギーと理論地震記象上からよみとった各周期の波の振幅の関係が第 15 図である．このうち case 5 はエネルギーを考えると case 3 の近くまで左に移すのが合理的である．図示の二本の直線に

$$Ms=\log A+Q \quad (Q=5.05,\ \Delta=90^\circ)$$

という表面波による規模を入れると

$$\log E=2.0\,M+7.32$$
$$\log E=2.0\,M+7.80$$

となる．

理論の示す所によれば，エネルギー E はモーメント M_0，従って振幅 A の二乗に比例する．この図から M_0 の代りに時間関数を替えても上の傾向が成り立つことが分ったので，理論的には $\log E$ と M の式の M の係数としては，2.0 をとることがよいと考えられる．グーテンベルグ・リヒターによる

$$\log E=1.5\,M+11.8$$

のエネルギーは，ここに示したエネルギーとは別の量を示すと考えられる．
9. ここで使うエネルギーは第 5 表の case 6 の場合 $E\propto M_0^2/t_r^3$ という関係にある．t_r は時間の次元を持つ量で震源でのプロセス時間又はそれと密接な関係をもつ量であるから M_0 と E がわかると t_r の見当をつけることができる．